

Advancing a Post-Anoxic Biological Nutrient Removal Process Selecting for Nitritation

A Thesis

Presented in Partial Fulfillment of the Requirements for the

Degree of Master of Science

with a

Major in Civil Engineering

in the

College of Graduate Studies

University of Idaho

by

Felicity J. Appel

Major Professor: Erik R. Coats, P.E., Ph.D.

Committee Members: James Moberly Ph. D.; Kevin Chang Ph.D.

Department Administrator: Robert Nielson Ph.D.

### Authorization to Submit Thesis

This thesis of Felicity J. Appel, submitted for the degree of Master of Science with a Major in Civil Engineering and titled "Advancing a Post-Anoxic Biological Nutrient Removal Process Selecting for Nitrification," has been reviewed in final form. Permission, as indicated by the signatures and dates below, is now granted to submit final copies to the College of Graduate Studies for approval.

Major Professor: \_\_\_\_\_ Date: \_\_\_\_\_  
Erik R. Coats, P.E., Ph.D.

Committee  
Members: \_\_\_\_\_ Date: \_\_\_\_\_  
James Moberly, Ph.D.

\_\_\_\_\_ Date: \_\_\_\_\_  
Kevin Chang, P.E., Ph.D.

Department  
Administrator: \_\_\_\_\_ Date: \_\_\_\_\_  
Richard J. Nielsen, P.E., Ph.D.

## **Abstract**

Wastewater is treated biologically with activated sludge to remove the nutrients phosphorous and nitrogen. In accomplishing wastewater treatment, selecting for nitrification in the aeration phase can optimize the nutrient removal process to conserve energy and carbon, while enhancing phosphorous and nitrogen removal. This thesis investigated the ability of sequencing batch reactors (SBRs), operated in a unique post-anoxic denitrification mode (process referred to as BIOPHO-PX; trademark under development by Dr. Coats), to remove nutrients while controlling aeration length and residual DO concentration at different solids retention times (SRTs), with the goal to induce and sustain nitrification. Phosphorus removal of 97% and nitrogen removal of 82% were achieved with this process configuration.

## **Acknowledgements**

Foremost I would like to acknowledge my major professor, Erik Coats Ph.D., whose support financially, academically and mentally made this thesis possible. Also I would like to acknowledge my committee members, James Moberly, Ph. D. and Kevin Chang, Ph. D., for their guidance in constructing this thesis.

I would also like to acknowledge Derek Probst and Jason Mellin, the other members of the BIOPHO-PX for the hard work and dedication to the BIOPHO-PX system and long days of cycling and sample collection.

Finally, I would like to acknowledge Cynthia Brinkman for her exceptional qPCR assistance as well as Trevor Woodland, Regan Hanson, Dmitriy Shimberg and Terrence Stevenson for their assistance during reactor comprehensive assessments.

## **Dedication**

To my husband Dan and our son River.

## Table of Contents

Authorization to Submit Thesis .....	ii
Abstract .....	iii
Acknowledgements .....	iv
Dedication .....	v
Table of Contents .....	vi
List of Figures .....	vii
List of Tables .....	ix
Chapter 1: Introduction and Background.....	1
Chapter 2: Literature Review.....	8
2.1 Nitritation versus Nitrification .....	8
2.2 Controlling for Nitritation.....	14
2.3 Denitritation versus Denitrification and Phosphorous Removal .....	20
Chapter 3: Experimental Design.....	25
Chapter 4: Methods.....	28
Chapter 5: Results and Discussion.....	32
5.1 10-Day SRT.....	32
5.1.1 Nitrogen Removal in Reactors with 10-day SRT.....	33
5.1.2 Phosphorous Removal in Reactors with 10-day SRT .....	40
5.1.3 DO Analysis for reactors at 10-day SRT .....	42
5.1.4 10-day SRT Specific Rates .....	44
5.1.5 Summary and Conclusions for Reactors at 10-day SRT.....	44
5.2 20-Day SRT.....	45
5.2.1 Nitrogen Removal in Reactors with 20-day SRT.....	46
5.2.2 Phosphorous Removal for Reactors at 20-day SRT .....	53
5.2.3 DO Analysis for Reactors at 20-day SRT .....	56
5.2.4 20-day SRT Specific Rates .....	57
5.2.5 Summary and Conclusions for Reactors at 20-day SRT.....	58
Chapter 6: Conclusions.....	60
6.1 Operational Recommendations.....	60
6.2 Energy Savings with Operational Recommendations .....	61
6.3 Future Investigations .....	61
Works Cited.....	63

## List of Figures

Figure 1: Pre-anoxic Configuration.....	3
Figure 2: Post-Anoxic Configuration.....	3
Figure 3: MLR versus Pre-anoxic % of Nitrate Removed.....	4
Figure 4: BIOPHO-PX Configuration.....	6
Figure 5: Diagram of AOB metabolism (Madigan and Martinko 2006).....	9
Figure 6: Diagram of NOB metabolism (Madigan and Martinko 2006).....	10
Figure 7: Monod growth kinetics for AOBs and NOBs (Blackburne, Yuan and Keller 2008) .....	11
Figure 8: Example of nitrification control using pH. Note break points and valleys in the DO and NH <sub>4</sub> curves, when nitrification was complete (J. Guo, et al. 2009).....	16
Figure 9: Example of OUR versus time over two aeration cycles (Lemaire, Marcelino and Yuan 2008).....	18
Figure 10: Diagram of typical PAO metabolism (Smulders, et al. 2004).....	22
Figure 11: Carbon and Phosphorous Cycling during EBPR in an SBR (Winkler, Coats and Brinkman 2011).....	23
Figure 12: Average BIOPHO-PX1 at 10 day SRT n=3.....	35
Figure 13: Average BIOPHO-PX 2 at 10 day SRT n=3.....	35
Figure 14: BIOPHO-PX 3 on a)10/1/14, b)10/9/14 and c)10/15/14, and d)Average BIOPHO- PX 3 Phosphorous and Nitrogen across the cycle n=3.....	38
Figure 15: BIOPHO-PX 4 on a) 10/1/14, b) 10/9/14 and c) 10/15/14, and d)Average BIOPHO-PX 4 Phosphorous and Nitrogen across the cycle n=3.....	39
Figure 16: Typical DO Profiles for BIOPHO-PX 1 through 4 at 10-day SRT, 10/16/2014....	43
Figure 17: BIOPHO-PX 1 on a)2/16/15, b) 3/7/15 and c)3/16/15, and d)Average BIOPHO- PX 1 Phosphorous and Nitrogen across the cycle n=3.....	49
Figure 18: BIOPHO-PX 2 on a) 2/16/15, b) 3/7/15 and c) 3/16/15, and d) Average BIOPHO- PX 2 Phosphorous and Nitrogen across the cycle n=3.....	50
Figure 19: BIOPHO-PX 3 on a) 2/16/15, b) 3/7/15 and c) 3/16/15, and d) Average BIOPHO- PX 3 Phosphorous and Nitrogen across the cycle n=3.....	51

Figure 20 a-d: BIOPHO-PX 4 on 2/16/15, 3/7/15 and 3/16/15, and Average BIOPHO-PX 4 Phosphorous and Nitrogen across the cycle n=3 .....	52
Figure 21: Carbon in BIOPHO-PX1 and 2 .....	55
Figure 22: Carbon in BIOPHO-PX 3 and 4 .....	56
Figure 23: DO Profile across the aeration period for the BIOPHO-PX reactors 3/6/15.....	57

## List of Tables

Table 1: AOB/NOB Kinetic Parameters (Metcalf and Eddy 2014, Regmi, et al. 2014, Jubany, et al. 2009).....	11
Table 2: Target DO concentration for Experimental Reactors.....	25
Table 3: Phase Length per Cycle.....	26
Table 4: Primary Solids Fermenter Liquor Characteristics .....	27
Table 5: Summary of Average Concentrations for BIOPHO-PX 1 through 4 at 10-day SRT .....	32
Table 6: Percent Removal for BIOPHO-PX Reactors at 10-day SRT .....	40
Table 7: qPCR analysis for 10-day SRT.....	40
Table 8: Average MLSS concentrations for BIOPHO reactors at a 10 day SRT n=3.....	42
Table 9: Ratio of Influent VFAs to P and Effluent P.....	42
Table 10: Average Residual DO concentrations over an aeration cycle and Aeration Length at the residual DO .....	43
Table 11: 10-day SRT specific rates .....	44
Table 12: Average Phosphorous and Ammonia Concentrations at 20-day SRT.....	45
Table 13: Percent Removal for BIOPHO-PX Reactors at 20-day SRT .....	53
Table 14: qPCR data for BIOPHO-PX 1 through 4 at 20 day SRT.....	53
Table 15: Average MLSS concentrations for reactors with 20-day SRT n=3.....	54
Table 16: Influent VFA: and P ratios and Effluent P 20-day SRT .....	55
Table 17: Average Residual DO Concentrations and Time at Residual DO for BIOPHO-PX reactors at 20-day SRT.....	57
Table 18: 20-day SRT specific rates .....	58

## Chapter 1: Introduction and Background

Municipal wastewater contains the inorganic nutrients phosphorous and nitrogen in the form of phosphate and ammonia. These nutrients must be removed from the wastewater stream before it is discharged into a receiving water body (river, lake, etc.) to prevent advanced surface water body eutrophication. Eutrophication is a natural phenomenon that can lead to an overgrowth of aquatic plants in a water body, which then causes hypoxia, or a decrease in dissolved oxygen, in the water body. This decrease of dissolved oxygen can result in the death of fish and other aquatic animals. In order to maintain a healthy ecosystem in the receiving body, phosphorous and nitrogen are removed in Water Resource Recovery Facilities (WRRFs).

In WRRFs, biological and/or chemical systems can be used to remove nutrients to appropriate, permitted concentrations. The chemical removal process uses the addition of expensive, synthetic chemicals, such as metal salts and polymers, to remove nutrients from the wastewater stream. Moreover, chemical WRRF processes have been shown to have an increased global warming potential of 13.2% at a full-scale WRRF (Coats, Watkins and Kranenburg 2011). While these treatment methods are excellent at removing nutrients, a central goal of the Coats research group is to reduce the environmental impact and operational cost of a WRRF. For these reasons, and based on previous research performed by this research group (Coats, Watkins and Kranenburg 2011), only biological processes are evaluated. Biological systems remove nutrients from influent wastewater stream through the use of an activated sludge process. The term “activated sludge” refers to a mixed microbial community growing in a mixed wastewater environment (referred to as suspended growth),

with the microbial community accomplishing removal of select components from the wastewater stream. When activated sludge systems are designed to target removal of nitrogen and phosphorous, the process is referred to as biological nutrient removal (BNR).

The basic, conventional BNR configuration (targeting carbon, nitrogen and phosphorus removal) consists of a series of three tanks containing activated sludge, with each tank engineered to provide a specific environment – anaerobic (AN), aerobic (AE), or anoxic (AX). The anaerobic environment is devoid of oxygen and nitrogen gases, while the anoxic environment is only devoid of oxygen gas. The aerobic environment is where aeration takes place and oxygen gas is introduced to the system. Depending on the nutrients that must be removed, the BNR systems will include some combination, or all, of these environments, ultimately enriching for bacteria capable of removing the target nutrients.

The configuration and use of these three environments affect how and what nutrients are removed from the wastewater stream. First, considering only an aerobic environment, WRRFs can achieve removal of carbonaceous material, represented as biological oxygen demand (BOD), through partial or complete oxidation by heterotrophic organisms. BOD removal is important as excess BOD can deplete the dissolved oxygen (DO) in the receiving body. Aerobic ammonia oxidation to nitrite/nitrate can also be achieved in an aerobic-only environment, along with BOD removal, by extending the solids retention time (SRT) in the system to allow for the growth of ammonia oxidizing bacteria (AOB). SRT is an operational parameter that represents, generally, the average age (and relative concentration) of biomass in a BNR system.

Total nitrogen removal can be achieved by the addition of an anoxic environment to an aerobic environment. Nitrogen species are measured on a nitrogen basis therefore they are

reported as “nitrate as nitrogen” ( $\text{NO}_3\text{-N}$ ) and similarly for the other nitrogen species. There are two different possible process configurations when nitrate-nitrogen removal is required as it can be toxic to aquatic species and humans in the receiving body of water: pre-anoxic and post-anoxic (Figure 1 and Figure 2, respectively).

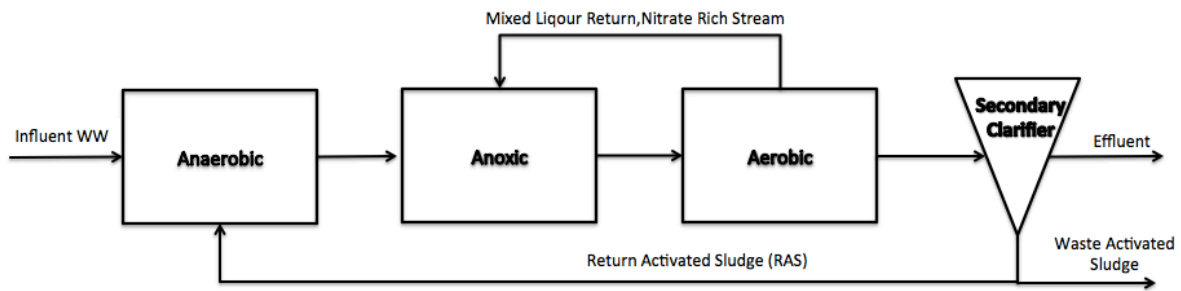


**Figure 1: Pre-anoxic Configuration**

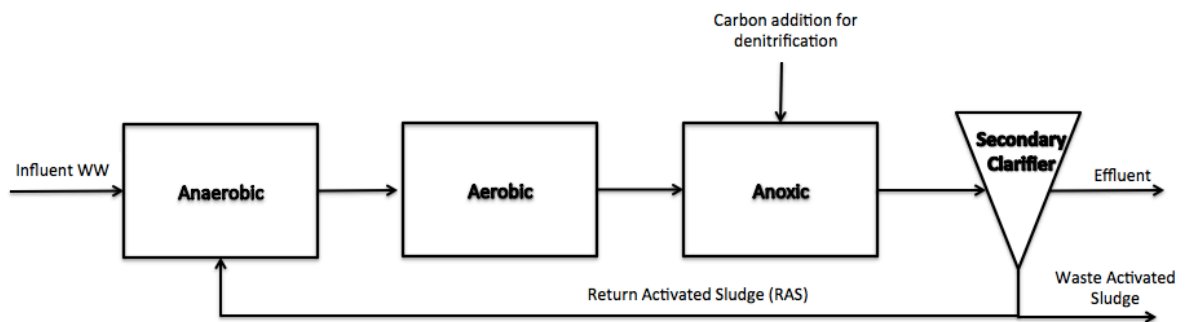


**Figure 2: Post-Anoxic Configuration**

The pre-anoxic nutrient removal process is configured with the waste stream first entering the anoxic zone followed by the aerobic zone. This configuration has the advantages of gaining alkalinity in the system and reducing the aeration demand by using nitrate instead of oxygen to oxidize the influent BOD. While the pre-anoxic configuration removes nitrate-N adequately, as shown the process requires an internal recycle (IR) stream, or mixed liquor return (MLR) stream, from the aerobic zone to the upgradient anoxic zone to achieve denitrification. The recycle stream pump increases the electricity demand, and therefore

operational cost, for a WRRF. The recycle stream can also cause denitrification problems by i) introducing dissolved oxygen into the anoxic zone, and ii) diluting the influent stream so that is not enough substrate available for the bacteria to perform denitrification. Pre-anoxic denitrification does not allow for the complete removal of nitrogen species because only part of the oxygenated stream containing nitrite or nitrate is recycled and the remainder is discharged as effluent from the WRRF. Figure 3 shows the percent of nitrogen removed from the waste stream as a function of the MLR. Even in the best circumstances and the highest MLR, only 90% of the nitrogen is removed, meaning the remaining 10% is discharged in the effluent into the receiving surface body.

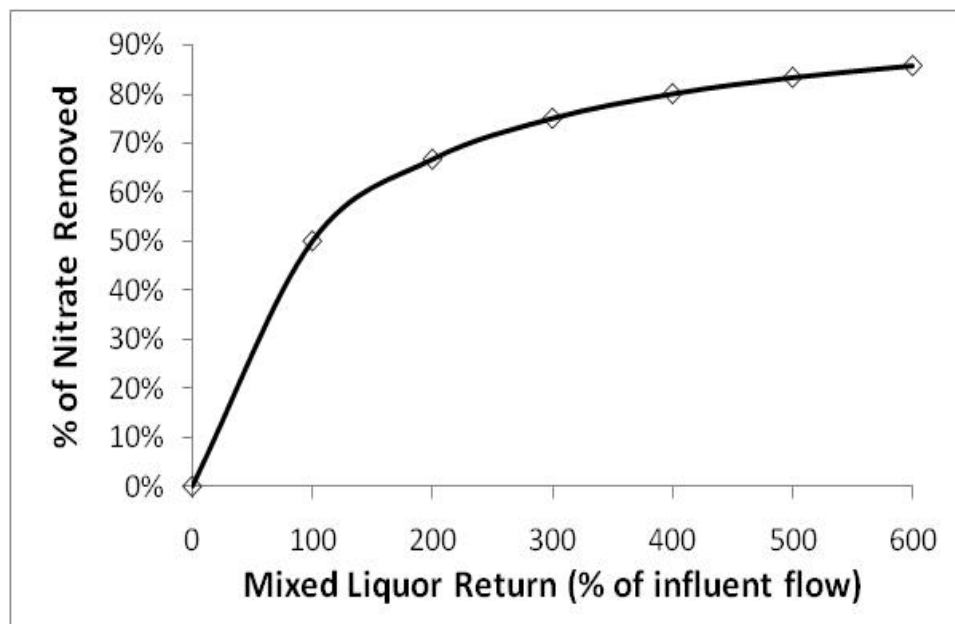


**Figure 3: MLR versus Pre-anoxic % of Nitrate Removed**

A post-anoxic denitrification configuration has the wastewater stream first entering the aerobic zone, followed by the anoxic zone. While this configuration does not require an internal recycle stream, it does typically require the addition of carbon (usually methanol) into the anoxic basin to achieve denitrification, which results in added costs (and adverse

environmental impacts) to the WRRF. The addition of carbon is required to achieve denitrification, as microorganisms responsible for denitrification require not only a carbon source for growth but also to utilize as an electron donor in the reduction of nitrite/nitrate to nitrogen gas (Metcalf and Eddy 2014).

The types of environments used in the activated sludge basin are also important for achieving enhanced biological phosphorus removal (EBPR). Specifically, the cycling of bacteria through anaerobic/aerobic environments is required to achieve EBPR, where the activated sludge enters the anaerobic environment before entering the aerobic zone (and the MLSS is cyclically processed through the anaerobic-aerobic zones, as shown in Figure 1). The addition of an anaerobic basin will allow for phosphorus removal and therefore a WRRF that can achieve BNR. The metabolisms and mechanisms for phosphorous removal are discussed in Section 2.0

In an attempt to decrease WRRF cost and increase nutrient removal efficiency from the conventional approaches discussed above, a novel post-anoxic process for nutrient removal, referred to as BIOPHO-PX (Figure 4), was investigated for its ability to remove nitrogen and phosphorous while achieving cost and energy savings over the conventional nutrient removal approach. The BIOPHO-PX process (trademark in process) has been developed by the Coats environmental engineering lab group at the University of Idaho (Coats, Mockos and Loge 2011, Winkler, Coats and Brinkman 2011), with the goal to concurrently reduce WRRF energy demands and enhance the capture of valuable resources from wastewater. Regarding WRRF energy demand, one of the most expensive, energy-intensive processes in a WRRF is the use of aeration in the aerobic treatment stage. BIOPHO-PX seeks to reduce aeration by sustaining an ammonia removal process known as

nitritation (described below), rather than nitrification (described below). Operational parameters to control the BIOPHO-PX process as a nitritation system was a primary focus of the researched conducted on this thesis. Previous research suggests nitritation systems have a reduced aeration demand compared to nitrification systems (J. Guo, et al. 2009, Guo, et al. 2008). BIOPHO-PX is operated as a post-anoxic system, so a recycle stream from mixed liquor is not required.

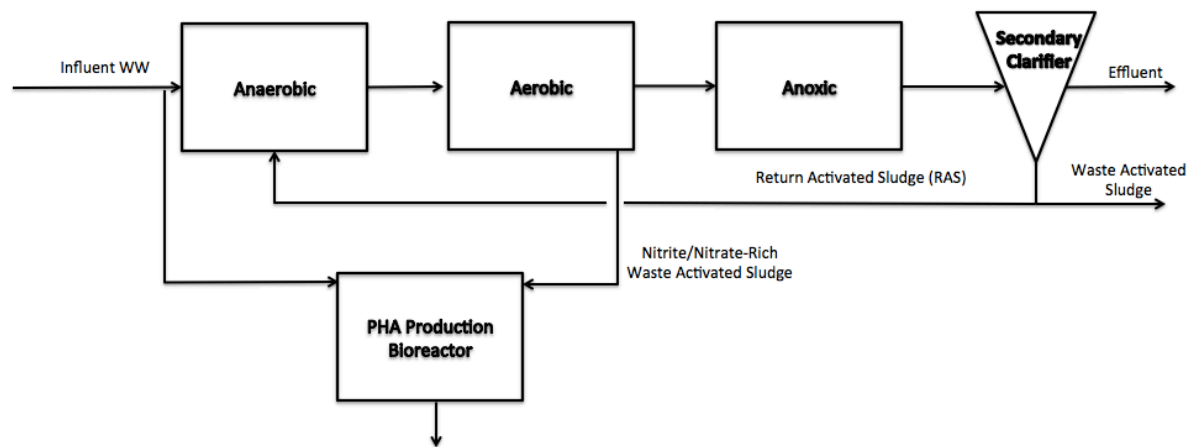


**Figure 4: BIOPHO-PX Configuration**

As we seek to achieve nutrient removal by employing biological processes, one of the most important constituents in wastewater is the organic carbon available in the system. The organic carbon facilitates, either directly or indirectly, the conversion and removal of all nutrients in the activated sludge system. The carbon can be in many forms, including suspended solids, volatile fatty acids (VFAs), glycogen, carbon dioxide, and carbohydrates. Microorganisms use these carbon sources to facilitate growth as well as to perform oxidation-reduction (redox) reactions to convert nutrients to compounds that can be removed by the organism from the bulk wastewater solution (Metcalf and Eddy 2014). Ultimately most municipal wastewater streams are carbon limited. However, within the context of

maximizing resource recovery from the wastewater, capturing carbon for products is of significant interest.

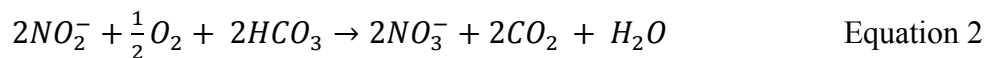
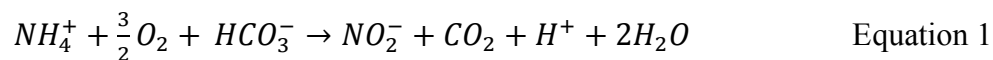
The BIOPHO-PX system employs specific environmental conditions to enrich for the growth of microorganisms that will store carbon internally and use it within appropriate environments to facilitate specific treatment needs. These microorganisms store carbon, removing it from the bulk solution, thus decreasing aeration demand and aeration costs. The microorganisms also may be harvested while full of the stored carbon (such as the bioplastic poly-hydroxyalkanoates (PHA)) and processed to remove the carbon so that it may be utilized for consumer products. With regard to the BIOPHO-PX configuration, nitritation has been shown to have a decrease in carbon demand of up to 40% compared to nitrification, which is examined on a thermodynamic level in further detail in section 2 (Regmi, et al. 2014, Daigger 2014). Carbon savings could then be captured elsewhere in the WRRF for additional nutrient removal or to be used as an additional resource, as mentioned above.

The purpose of the research conducted and described in this thesis was to investigate the optimization of nitritation in the BIOPHO-PX configuration to conserve carbon for downstream resource recovery, reduce the amount of energy used at a WRRF, and eliminate the need for the addition of external carbon sources for denitrification commonly associated with post-anoxic denitrification.

## Chapter 2: Literature Review

### 2.1 Nitritation versus Nitrification

In the biological process of removing nitrogen from wastewater, the first step is the oxidation of ammonium (NH<sub>4</sub>) to nitrite/nitrate. The biochemical reaction is realized in the two-step, microbially-mediated nitrification process shown in equations 1 and 2 (Metcalf and Eddy 2014). In complete nitrification, NH<sub>4</sub> is first oxidized to produce nitrite (NO<sub>2</sub>), a step known as nitritation or partial nitrification (as shown in Equation 1). In the second step, shown in Equation 2 and which completes the nitrification process, the nitrite is oxidized to produce nitrate (NO<sub>3</sub>). While nitrification has been a successful process historically utilized for the removal of ammonia from wastewater, ultimately, the removal of nitrogen only requires nitritation. The difference and similarities of the two operational processes, as well as the challenges to achieving only nitritation, are detailed below.



The oxidation of NH<sub>4</sub> to NO<sub>2</sub>, as shown in Equation 1, is performed by autotrophic bacteria known AOBs. Bacteria classified as AOBs include, *Nitrosomonas* and *Nitrospira* (Metcalf and Eddy 2014). AOBs use carbon dioxide (CO<sub>2</sub>) as their carbon source and NH<sub>4</sub> as the electron donor. The oxidation of ammonia using *ammonia monooxygenase* enzyme (AMO) is how AOBs derive their ATP energy, leveraging the ATP synthase mechanism and is associated with the proton motive force (Taher and Chandran 2013). The electron acceptor that is reduced during ammonia oxidation is oxygen (O<sub>2</sub>), which indicates that the AOBs are only active in an obligate aerobic environment such as the aeration basins

of a WRRF. Figure 5 illustrates the electron donor-electron acceptor metabolism of AOBs. As shown, AMO is a membrane-bound protein. This is also the enzyme that gives AOBs a higher DO affinity over Nitrite Oxidizing Bacteria (NOB) as it requires oxygen to perform ammonia oxidation. Two exogenously supplied electron and two hydrogen protons are needed along with AMO to oxidized  $\text{NH}_4$  to  $\text{NO}_2$ . These electrons are supplied to AMO via *cytochrome c* (cyt c) enzyme, which requires the reduction of oxygen. NOBs also utilize this enzyme (Madigan and Martinko 2006).

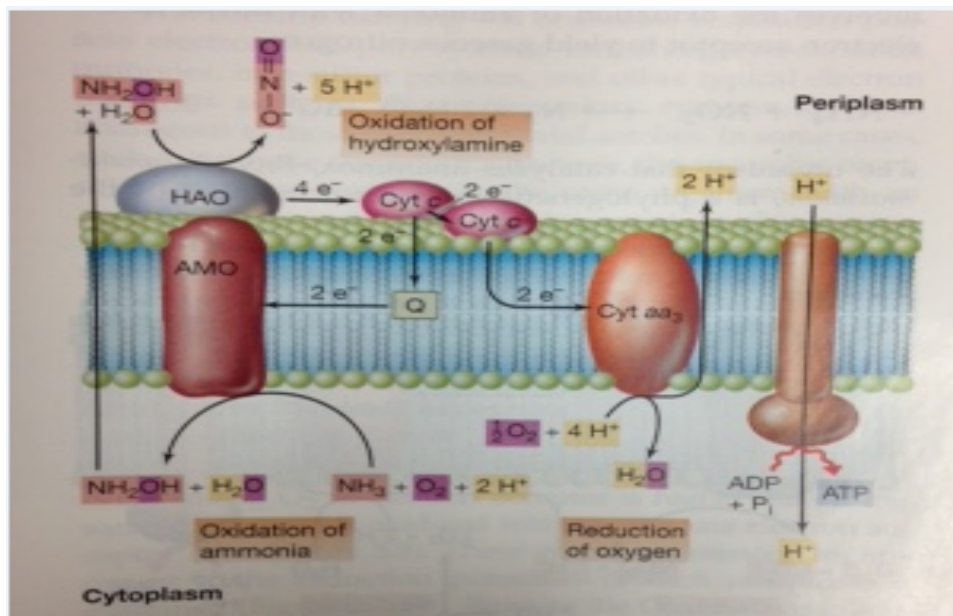


Figure 5: Diagram of AOB metabolism (Madigan and Martinko 2006)

For the oxidation of  $\text{NO}_2$  to  $\text{NO}_3$ , the autotrophic NOBs are active. Bacteria classified as NOBs include *Nitrobacter*, *Nitrococcus*, *Nitrospina* and *Nitrospira*. Similar to AOBs, NOBs use  $\text{CO}_2$  as their carbon source and  $\text{O}_2$  as the electron acceptor. NOBs use  $\text{NO}_2$  as the electron donor, which is oxidized using *nitrite oxidoreductase* (NOR). As with the AOBs, NOBs are also only active in an aerobic environment (Metcalf and Eddy 2014). Figure 6 shows a diagram of NOB metabolism. *Cytochromes* types a and c are present to transport

electrons (Madigan and Martinko 2006). Oxygen is only utilized by cyt c which gives NOBs a lower oxygen affinity than AOBs as AOBs require oxygen for cyt c and AMO.

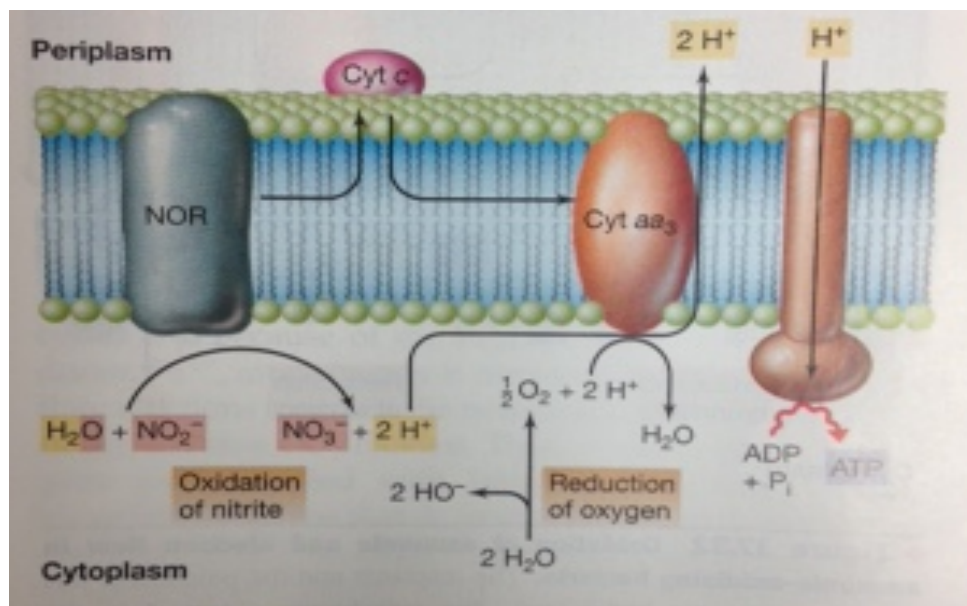


Figure 6: Diagram of NOB metabolism (Madigan and Martinko 2006)

Monod growth kinetic models are used to describe the presence, performance, and function of AOBs and NOBs in a biological treatment system. Figure 7 shows how the dissolved oxygen concentration affects the growth of AOBs and NOBs. The specific growth rate of AOBs and NOBs is a function of the species being oxidized ( $\text{NH}_4$  versus  $\text{NO}_2$ ), the endogenous decay rate of the microorganism, and the DO concentration in the aeration basin. Monod growth models for AOBs and NOBs are shown in Equation 3 and 4, respectively, where  $\mu_{max}$  is the maximum specific growth rate,  $S_x$  is the initial concentration of  $\text{NH}_4$ ,  $\text{NO}_2$ , or DO in the system,  $K_x$  is the half saturation coefficient (or the concentration of the substrate when the growth rate is half of the maximum growth rate) and  $b$  is the specific endogenous decay rate of the microorganisms. Table 1 shows typical values for the kinetic parameters. These values are dependent on the oxygen transfer limitations of the sludge itself and therefore vary from system to system (Blackburne, Yuan and Keller 2008).

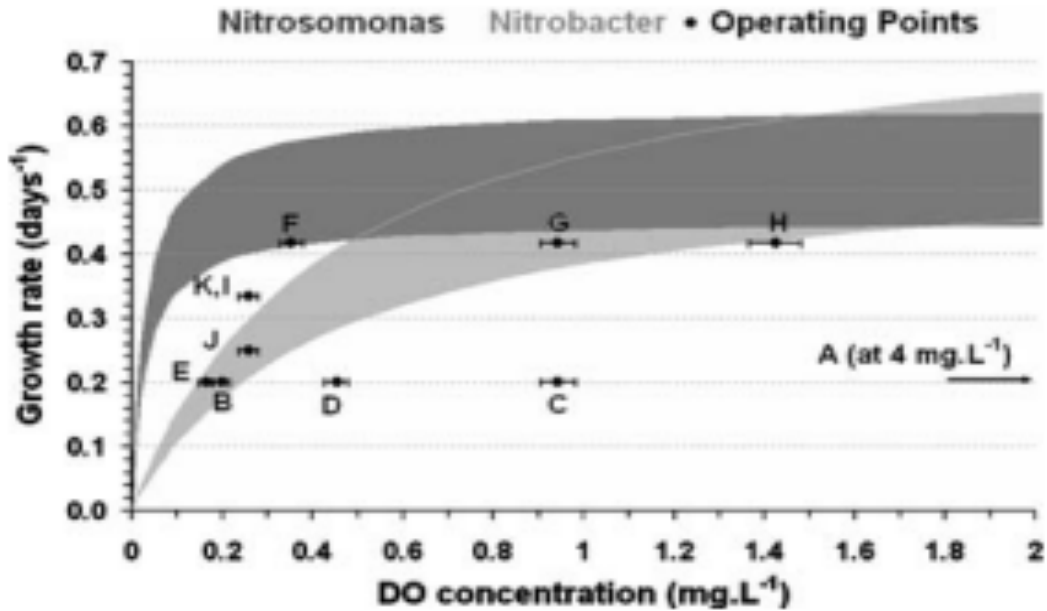


Figure 7: Monod growth kinetics for AOBs and NOBs (Blackburne, Yuan and Keller 2008)

$$\mu_{AOB} = \mu_{max,AOB} \left( \frac{S_{NH}}{S_{NH} + K_{NH}} \right) * \left( \frac{S_o}{S_o + K_{o,AOB}} \right) - b_{AOB} \quad \text{Equation 3}$$

$$\mu_{NOB} = \mu_{max,NOB} \left( \frac{S_{NO}}{S_{NO} + K_{NO}} \right) * \left( \frac{S_o}{S_o + K_{o,NOB}} \right) - b_{NOB} \quad \text{Equation 4}$$

Table 1: AOB/NOB Kinetic Parameters (Metcalf and Eddy 2014, Regmi, et al. 2014, Jubany, et al. 2009)

Coefficient	Units	Range
$\mu_{AOB}$	g VSS/g VSS*day	0.33 - 1.05
$\mu_{NOB}$	g VSS/g VSS*day	1.0 - 1.8
$K_{o,AOB}$	mg/L	0.14 - 1.16
$K_{o,NOB}$	mg/L	0.05 - 0.2

Comparing AOB and NOB kinetics, AOBs exhibit a lower maximum growth rate over all compared with NOBs but have a higher growth rate at low DO concentrations (Table 1 and slopes of growth curves in Figure 7). In order to inhibit or minimize the relative fraction of NOBs in the activated sludge environment (a central goal of this research), conditions must be established that favor AOB kinetics (Metcalf and Eddy 2014). The lower half-saturation constant for NOBs also indicates a steeper growth curve when compared to

AOBs. Research has shown that AOB growth is favored and NOB growth can be hindered at low DO concentrations due to AOBs higher affinity for oxygen in low DO environments (Regmi, et al. 2014, W. Zeng, et al. 2009, Metcalf and Eddy 2014). AOBs' affinity for  $\text{NH}_4$  ( $K_{\text{NH}_4, \text{AOB}} = 9.1$ ) has been found to be higher than the affinity of NOBs for  $\text{NO}_2$  ( $K_{\text{NO}_2, \text{NOB}} = 4.85$ ) at low DO concentrations, which also lends to AOB kinetic being more favorable (Fang, et al. 2009). The oxidation rate of  $\text{NO}_2$  by NOBs is more hindered at low DO concentrations than the oxidation rate of  $\text{NH}_4$  by AOBs (Metcalf and Eddy 2014). The specifics of how to achieve DO control for nitrification are discussed in the following section.

Controlling an activated sludge system to operate at a low DO concentration affects the microorganism populations present in system. As stated above, at low DO concentrations the AOBs have a higher affinity for DO than NOBs (Regmi, et al. 2014, W. Zeng, et al. 2010, Lemaire, Marcelino and Yuan 2008, W. Zeng, et al. 2009). This means that AOBs will outcompete NOBs for the DO, controlling how much DO is left available to NOBs. As noted, generally there are two genus of NOBs considered to predominate activated sludge: *Nitrobacter* and *Nitrospira* (Metcalf and Eddy 2014, Huang, et al. 2010). At low DO concentrations *Nitrobacter* growth is inhibited in an activated sludge system. *Nitrospira* growth is inhibited when nitrite accumulates in the system, i.e. when the system is optimized for nitrification. This inhibition is due to the increase of free ammonia ( $\text{NH}_3$ ) and free nitrous acid ( $\text{HNO}_2$ ) that forms in the system as nitrification occurs and the pH subsequently falls (Jubany, et al. 2009). As the pH decreases from the release of hydrogen ions, nitrite is formed, and free ammonia and free nitrous acid become more prevalent in the systems. The lack of DO for NOBs and the accumulation of  $\text{NO}_2$  in the system can contribute to NOB

inhibition or washout from the microorganism community (Jubany, et al. 2009, Huang, et al. 2010).

As described in Section 1.0, the reduction of  $\text{NO}_2$  and  $\text{NO}_3$  in an activated sludge system, with both nitrogen species produced via nitrification/nitrification within the aerobic environment, occurs in the anoxic zone of a BNR WRRF, where the two nitrogen species serve as terminal electron acceptors. Beyond reducing oxygen demand (and realized associated energy savings), there is another benefit to controlling  $\text{NH}_4$  oxidation at  $\text{NO}_2$ , specifically as related to conserving wastewater carbon. As terminal electron acceptors, the relative theoretical energy generated between the two nitrogen species is significantly different. When a biochemical reaction occurs, for example the reduction of  $\text{NO}_2$  to nitrogen gas, there is a change in energy that can be quantified thermodynamically by the Gibbs free energy ( $\Delta G^\circ$ ) at standard conditions of  $\text{pH} = 7.0$  and a temperature of  $25^\circ\text{C}$ . The Gibbs free energy describes the transfer of 1 mole of electron in oxidation-reduction and synthesis reactions. For reactions that have a negative  $\Delta G^\circ$  value, energy is released into the system, and the reactions are recognized as being exergonic. These reactions will proceed spontaneously and do not require any input energy to proceed. The energy released from these reactions can be used for cell growth and other cellular functions within the biological system. Comparing the Gibbs free energies, as an electron acceptor  $\text{NO}_2$  has a  $\Delta G^\circ$  value of  $-93.23$  kJ/electron equivalent, while  $\text{NO}_3$  has a  $\Delta G^\circ$  value of  $-71.67$  kJ/electron equivalent when it is used as an electron acceptor. Because the  $\Delta G^\circ$  value of  $\text{NO}_2$  is more negative, the reaction is more exergonic and therefore more energy will be released when it is used as an electron acceptor. The greater release of energy will allow for a greater biomass yield for a given quantity of electron donor (e.g. VFAs), making it more valuable than  $\text{NO}_3$

in biological system (Metcalf and Eddy 2014), and also in the BIOPHO-PX system. More specifically, because of the greater release of energy into the system, less wastewater carbon will be needed to achieve denitrification (reduction of  $\text{NO}_2$  to nitrogen gas) than denitrification (reduction of  $\text{NO}_2$  to nitrogen gas). It has been shown that denitrification requires 40% less carbon than denitrification (Daigger 2014). As envisioned in the BIOPHO-PX process, this carbon savings can be utilized in a side stream process wherein excess VFAs are stored as the bioplastic polyhydroxyalkanoate (PHA) which is then recovered as a commodity.

## 2.2 Controlling for Nitrification

As discussed, controlling  $\text{NH}_4$  oxidation to stop at  $\text{NO}_2$ , represents an opportunity to reduce WRRF operational costs in the aerobic environment, while conserving carbon for production of a secondary commodity (e.g. PHA) in the anaerobic environment. In the aeration basin, there are several operational variables that may be controlled to select for the nitrification process. These variables include the length of time that air is applied to the system (aeration length), residual DO concentration, and SRT Parameters such as N-species concentrations, oxygen uptake rate (OUR), and/or pH can also be monitored in real-time and used to regulate the aeration length, and thus control for nitrification. Ultimately, some of these real-time monitoring methods measure one or more surrogates of metabolic activity that relate to nitrification.

Controlling the length of the aeration period may be a simpler approach to sustaining nitrification. A predetermined aeration length can be used when air is diffused into the systems, with or without online monitoring of constituents inside the aeration system (detailed below). If online monitoring is employed, aeration length can be controlled by DO set points (see setpoints discussion below). When a setpoint is reached and is detected by the online

monitoring probes, the air can be turned off and the aerobic phase is completed (with mixers activated to ensure the activated sludge remains suspended in solution). A decreased aeration length would correspond to decreased energy savings for a WRRF because less air would be required and therefore less pumping time and electricity used.

In considering setpoints for online aeration control, the following parameters could be measured in real-time to control for the length of time that air is applied to the system:  $\text{NH}_4$ ,  $\text{NO}_2$ , and  $\text{NO}_3$  concentrations. Commercial instrumentations are available for all the inorganic parameters: for example, Unisense  $\text{NO}_2$  and  $\text{NO}_x$  biosensor probes, Spectrolyzers for  $\text{NO}_2$  and  $\text{NO}_3$ , Hach  $\text{NO}_3$  ion selective electrodes, and AMTAX  $\text{NH}_4$  probe. Each constituent can be measured semi-continuously and a set ratio of desired effluent concentrations programmed into the monitoring system. Success has been observed with an effluent concentration setpoint for  $\text{NH}_4\text{-N}$  of 1.5 mg/L and a setpoint ratio of 1:1 for  $\text{NH}_4\text{-N}$  and  $\text{NO}_x\text{-N}$ . In those investigations, if the  $\text{NH}_4\text{-N}:\text{NO}_x\text{-N}$  ratio was higher than the set point, the system would aerate. Conversely, if the ratio were too low air would shut off until the ratio was restored. This operational condition continued until the  $\text{NH}_4$  concentration was 1.5 mg/L when the aerobic phase of treatment was ended (Regmi, et al. 2014). The disadvantage of this approach is the reliability of the probes being used. Constant calibration would need to be performed to ensure correct readings.

During nitrification, hydrogen ions are produced (equation 1) which lowers the pH of the mixed liquor (Li, et al. 2014); thus online pH monitoring is a potential surrogate method for controlling and monitoring nitrification. In monitoring pH in real-time, the slope of the pH versus time curve changes from negative to a positive slope when the  $\text{NH}_4$  has been completely oxidized to  $\text{NO}_2$ , which can be seen as a “valley” in the curve (Guo, et al. 2008,

Lemaire, Marcelino and Yuan 2008, W. Zeng, et al. 2009, W. Zeng, et al. 2010). An example of this can be seen in Figure 8. When this change in slope is detected, aeration can be shut off, ending the aeration period, with the assumption that nitrification has been achieved. This method of aeration length control is potentially easy to use, as pH probes are not a specialty item. However, the “valley” in the pH curve may be difficult to detect in some systems, which could result in overshooting of the “valley” by the monitoring software and over aeration. The disadvantage of this method of aeration control is the sensitivity of the system. If the instrumentation is too sensitive it could prematurely detected the ammonia valley. Conversely, if the system is not sensitive enough the ammonia valley may not be detected and the system will over-aerate, thereby losing nitrification control. Another disadvantage is that the pH of a full-scale WRRF is variable through out the day and may decrease for reasons unrelated to nitrification and may cause false valleys in the pH curves.

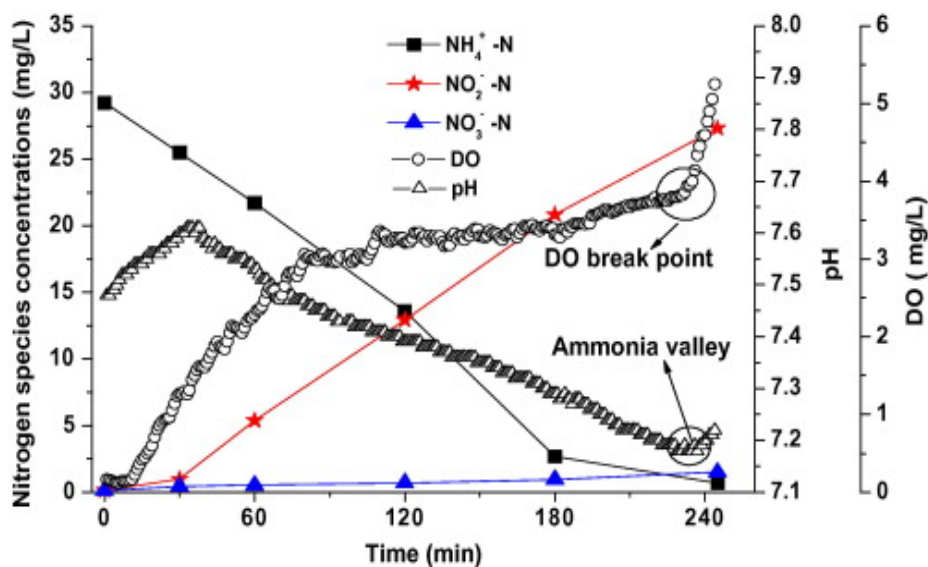


Figure 8: Example of nitrification control using pH. Note break points and valleys in the DO and  $\text{NH}_4$  curves, when nitrification was complete (J. Guo, et al. 2009)

Recognizing the importance of oxygen in nitritation/nitrification, the oxygen uptake rate (OUR) could be used in real-time to indicate when ammonia oxidation to  $\text{NO}_2$  has been completed. The OUR is the calculated rate at which an activated sludge system uses dissolved oxygen. OUR monitoring would involve calculating the change in the residual DO in the system over a set time interval (Katipoglu-Yazan, Cokgor and Orhan 2015, Lemaire, Marcelino and Yuan 2008). Using online monitoring, a significant decrease in the downward slope should be observed in the OUR versus time curve when ammonia oxidation to nitrite is complete (see Figure 9 as an example). When this sharp decrease in slope is detected it can be assumed that  $\text{NH}_4$  has been oxidized to  $\text{NO}_2$  and the air can be turned off. As an example of this method of nitritation control, a setpoint of  $1.2 \text{ mg O}_2 \text{ L}^{-1} \text{ min}^{-1}$  has been shown to be effective in nitritation control; when the OUR was lower than this set point, the aeration was switched off (Lemaire, Marcelino and Yuan 2008). This resulted in complete  $\text{NH}_4$ -N oxidation and effluent  $\text{NO}_x$ -N concentrations of 0.9-1.6 mg/L with 81-92% nitrite accumulation (i.e. 81-92% of measured oxidized  $\text{NH}_4$ -N was measured as  $\text{NO}_2$ -N) (Lemaire, Marcelino and Yuan 2008). The disadvantage of this method is that the OUR is dependent on the temperature of the waste stream. A decrease in the temperature by 10 degrees corresponds to a drop in the OUR by approximately 50%, which results in necessary aeration rate reduction (Wett, et al. 2010). Therefore the setpoint would need to be adjusted as the temperature changes which could confound this real-time nitritation control method.

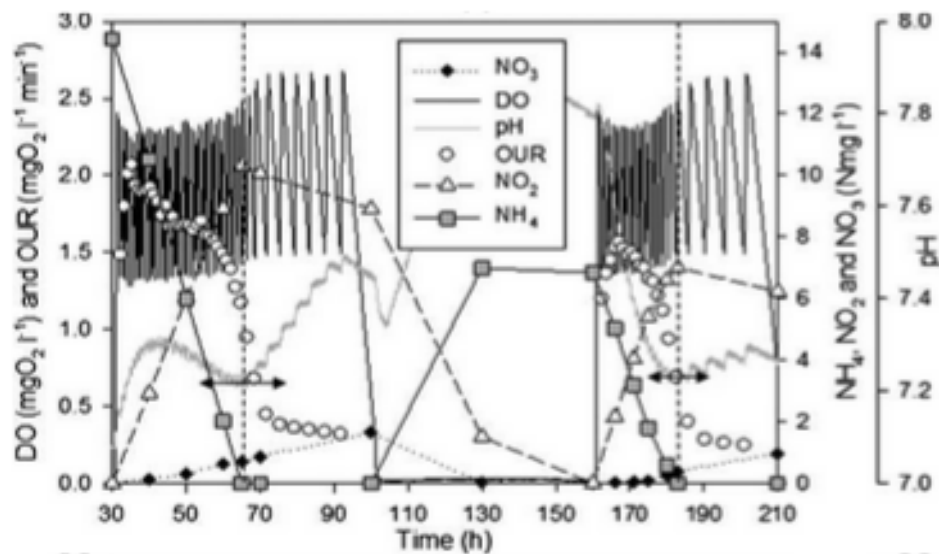


Figure 9: Example of OUR versus time over two aeration cycles (Lemaire, Marcelino and Yuan 2008)

As described above, DO in wastewater is required for the function of AOBs and NOBs. Conventional aeration basins that achieve complete nitrification maintain a residual or measurable DO concentration of at least 2 mg/L (Metcalf and Eddy 2014). Literature shows that a low (less than 2 mg/L) DO concentration can potentially select for nitritation over nitrification. For example, DO concentrations as low as 0.1–0.8 mg/L have been observed to achieve successful nitritation control by inhibiting NOB activity based on Monod growth kinetic models, shown in Equations 3 and 4 and in Figure 7 (J. Guo, et al. 2009, Li, et al. 2014, W. Zeng, et al. 2009, W. Zeng, et al. 2010). In this regard online monitoring of DO concentration in a reactor shows a “breakpoint” where there is a significant increase in the slope of the DO versus time curve; before this inflection point, the DO curve trends upwards (see Figure 8). This “breakpoint” can potentially be used to indicate when nitritation is achieved as it corresponds to the “valley” in the pH versus time curve where the pH follows a similar trend as the DO curve (Figure 8). These “breakpoints” or “valleys” can be used to indicate that the ammonia has been fully oxidized to nitrite (J. Guo, et al. 2009). Specifically,

a monitoring system can be utilized to record the DO curve and its slope. When a concurrent significant increase in both the DO slope and the DO occurs, the monitoring system would shut off the air, ending the aeration period. The advantage of this type of nitrification control is that DO can be maintained low so that only the required amount of air is introduced into the system to achieve nitrification, which could potential save on energy costs. The disadvantage is the monitoring system may not be sensitive enough to accurately detect the “breakpoint,” and the system will over-aerate and induce nitrification.

Online DO monitoring cannot only be used for controlling aeration length but it can also be used to control the aeration rate (amount of air introduced into the system) to maintain the DO in the system at a desired concentration (W. Zeng, et al. 2010). In fact, online DO monitoring is commonly employed at full-scale WRRFs (albeit not yet used for nitrification control). Employing this method as the monitoring system indicates that DO concentration is beginning to rise above a setpoint (indicating a decrease in electron donor substrate), the aeration rate can be reduced accordingly. Conversely, as the DO concentration decreases below a setpoint (indicating an increased availability of electron donor substrate), the aeration rate can then be increased. In contrast to aeration control discussed above, the air can also be provided intermittently during the aerobic period to ensure the DO concentration remains within a set range (Lemaire, Marcelino and Yuan 2008). This approach to nitrification control provides even greater control than monitoring for the “breakpoint,” as this method ensures over-aeration does not occur and air is not unnecessarily pumped into the system. However, this method does not monitor surrogate metabolic parameters that would indicate that ammonia oxidation to nitrite is complete which could lead to nitrate formation as well.

Managing the SRT presents a final potential mechanism to influence and/or control for nitrification. Generally, SRT is the average length of time that a microbe remains in the activated sludge WRRF, typically measured in days. The longer microbes remain in a system, the longer the SRT, and the WRRF MLSS concentration realizes a commensurate increase. Due to the fact that AOBs have a much slower growth rate than NOBs, longer SRTs, in fact, are needed to enrich the microbial population for AOBs (Metcalf and Eddy 2014). Previous research suggests successful nitrite accumulation at SRTs from 9-35 days (Li, et al. 2014, W. Zeng, et al. 2009, Jubany, et al. 2009). Ultimately, while SRT is not a real-time parameter that can be employed to control nitrification, the operational parameter is nonetheless critical in the overall nitrification process. This mechanism however must be used in conjunction with another method mentioned above to select for AOBs over NOBs.

### **2.3 Denitrification versus Denitrification and Phosphorous Removal**

After ammonia has been oxidized to  $\text{NO}_2$  and/or  $\text{NO}_3$ , it can then be reduced to nitrogen gas ( $\text{N}_2$ ), an inert gas that evolves from the WRRF into the atmosphere to complete nitrogen removal from the activated sludge. If nitrification is achieved nitrate is first reduced to nitrite, which is then reduced to nitrogen gas (Daigger 2014). With nitrification, the first reduction step is eliminated and only one reduction step is required, nitrite to nitrogen gas. The reduction of  $\text{NO}_2/\text{NO}_3$  (denitrification/denitrification) is performed by heterotrophic organisms in an anoxic environment (see previous discussion in Section 1.0). In order for this redox reaction to occur, sufficient organic carbon must be present to be used by the heterotrophs. In a conventional post-anoxic system that performs denitrification, an additional carbon source (such as methanol) must be added to drive denitrification or denitrification (see Figure 2). With the BIOPHO-PX system (Figure 4), as described, the goal

is to stop the ammonia oxidation process at nitritation; by controlling at nitrite and reducing the number of steps to reach nitrogen gas, carbon requirements in the anoxic environment are reduced by approximately 40% (Daigger 2014). This means that the microorganisms in a nitritating system, integrated with EBPR associated with the BIOPHO-PX process, would require 40% less carbon to perform redox reactions than microorganisms in a nitrification system. Due to the reduction in carbon demand, the microorganisms can utilize their conserved intracellular carbon stores to perform denitritation and therefore no external carbon is needed.

There are two general types of intracellular/internal carbon storage sources: glycogen and PHA; these carbon sources can be used by certain microorganisms enriched in an EBPR configuration for nitrite/nitrate reduction. These internal carbon sources are essential for biological nitrogen and phosphorus removal. Glycogen and PHA are used by heterotrophic bacteria to facilitate the reduction of nitrite/nitrate to nitrogen gas (denitritation/denitrification) and the uptake of phosphorus from the bulk solution (EBPR) (Metcalf and Eddy 2014, Daigger 2014, Lemaire, Marcelino and Yuan 2008). If microorganisms do not have enough carbon available they will not perform nutrient removal because they must conserve the carbon for their own cellular maintenance. The details of how they are used in heterotrophic metabolisms are detailed below.

Nitrogen removal is linked to phosphorous removal, within the context of the BIOPHO-PX process, as related to the internal carbon stores of heterotrophic organisms that can be used for denitritation/denitrification as mentioned above. During the anaerobic phase phosphorous is released into the bulk solution by the heterotrophic organisms known as Phosphate Accumulating Organisms (PAOs). Figure 10 shows a metabolic diagram of a

typical PAO. In the anaerobic environment PAOs release phosphorus into the bulk wastewater stream by breaking down intracellular poly-phosphate (poly-P) and glycogen, and consuming influent VFAs to produce PHA stores. Next the bacteria enter the aerobic phase where they oxidize the PHA previously stored to replenish their glycogen reserves and remove the  $\text{PO}_4\text{-P}$  from the bulk waste stream for poly-P storage. Figure 11 shows an example of the carbon (intra- and extracellular) and phosphorus cycling in the activated sludge system, based on a sequencing batch reactor. Phosphorus is then removed from the system when the PAOs are removed via waste activated sludge (Metcalf and Eddy 2014, Winkler, Coats and Brinkman 2011).

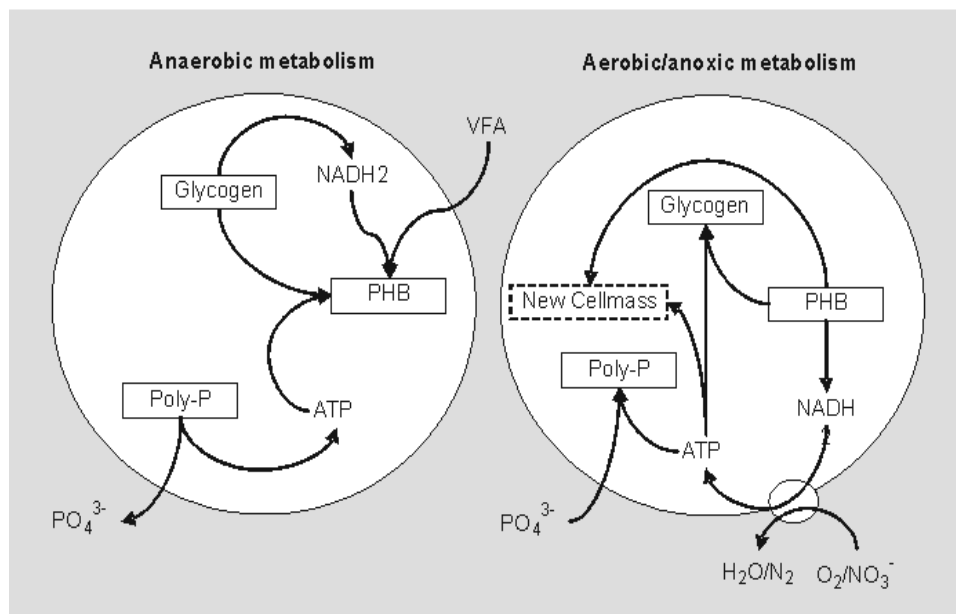


**Figure 10: Diagram of typical PAO metabolism (Smulders, et al. 2004)**

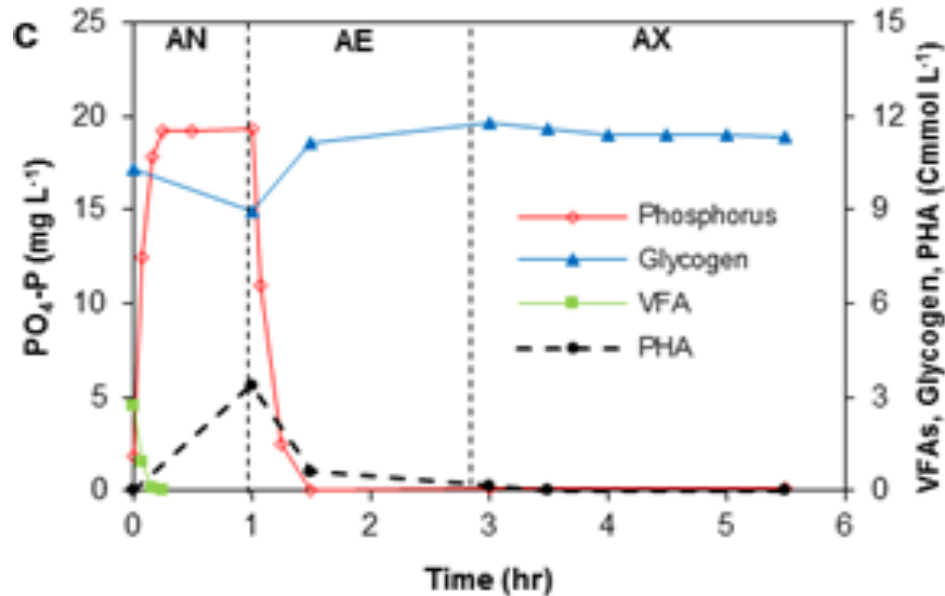


Figure 11: Carbon and Phosphorous Cycling during EBPR in an SBR (Winkler, Coats and Brinkman 2011)

There are generally considered to be two types of PAOs in an EBPR activated sludge system: standard PAOs and denitrifying PAOs (DNPAOs). DNPAOs can use their internal carbon stores to reduce nitrite/nitrate in the anoxic zone by using nitrite/nitrate as an electron acceptor. By using nitrite/nitrate as the electron acceptor DNPAOs are capable of removing phosphorous anoxically (Zeng, Yang, et al. 2011). DNPAOs are also able to use oxygen as an electron acceptor in the aerobic zone like a standard PAO (Lee and Yun 2014, Kapagiannidis, Zafiriadis and Aivasidis 2013, Soejima, Oki and Terada 2006).

Beyond PAOs, there is a group of microorganism that can potentially affect phosphorus removal adversely; this group is known as a Glycogen Accumulating Organisms (GAOs). These microorganism uses all of the same substrates as PAOs and perform similar overall metabolisms, so they are in direct competition for the “food;” however, GAOs do not remove phosphorus from bulk solution. If there is an excess of GAOs in the system, they may out-compete the PAOs for VFAs, which would limit the amount of phosphorus that can

be removed from the system (Metcalf and Eddy 2014). Denitrifying GAOs (DNGAOs) that remove nitrogen in the anoxic zone by using their internal glycogen stores as the carbon source (Liu, et al. 2013). While GAO populations can potentially impair the EBPR process, it is not clear how, or if, GAOs might affect the targeted denitrification metabolisms associated with the BIOPHO-PX process.

In order to maintain effective phosphorus removal, the activated sludge BPR system should be optimized for PAOs over GAOs. This can be achieved through control of residual dissolved oxygen, nitrite concentration and carbon sources available. Like AOBs and NOBs, DO affects the growth rate of PAOs and GAOs. PAOs have a higher affinity for oxygen than GAOs, so at low dissolved oxygen concentrations GAO growth will be inhibited (Carvalheira, et al. 2014). Nitrite concentration in an activated sludge system will also affect the PAO and GAO populations. As the nitrite concentration increases, GAO growth is inhibited which enriches the system for PAOs (Taya, et al. 2013). If phosphorous removal in the anoxic zone is required, nitrite concentrations over 20 mg/L can decrease GAO activity (Zeng, Yang, et al. 2011). A nitrification system (such as our BIOPHO-PX process) should expect a higher PAO population than GAO population.

Carbon sources present also affect the microorganism populations; specifically the relative distribution of acetic and propionic acid, which are common VFAs in an activated sludge system can facilitate selection of PAOs. PAOs can switch between acetic acid and propionic acid while maintaining equivalent carbon uptake rates, unlike GAOs, whose growth is inhibited if the substrate is changed (Oehman, et al. 2005). Therefore, PAOs are enhanced in the system over GAOs if the acetic to propionic ratio is between 75:25 and 50:50 (Lopez-Vazquez, et al. 2009).

### Chapter 3: Experimental Design

The purpose of this research was to optimize sequencing batch reactors (SBRs) using DO and aeration length to control for nitrification in the BIOPHO-PX process configuration. Investigations were conducted to evaluate the effects of nitrification control on nutrient removal within the BIOPHO-PX process configuration.

The investigations were conducted using 4 SBRs, each with 2-L working volumes. The reactors were inoculated from a first generation BIOPHO-PX reactor that had been inoculated from the Moscow, ID WRRF. The reactors were placed on magnetic stir plates to provide mixing. To establish and evaluate the effects of DO concentration and aeration length on nitrification control, high and low DO set points were chosen and assigned to each of the reactors. The set points were determined after reviewing literature that identified potential DO concentrations necessary to achieve nitrification and/or inhibit NOB growth/function (J. Guo, et al. 2009, Regmi, et al. 2014, Metcalf and Eddy 2014) and are listed in Table 2. The reactors were operated on 6-hour cycles controlled by a PLC. The lengths of each environment (anaerobic, aerobic, anoxic) within the cycle are listed in Table 3. At the beginning of each cycle, 0.67 L of wastewater was fed to each reactor; resulting in a hydraulic retention time (HRT) of 18 hr. Biomass was wasted automatically from each reactor at the end of the aerobic phase to maintain the target SRT. The feeding, decanting, and wasting were performed by peristaltic pumps controlled by the PLC.

**Table 2: Target DO concentration for Experimental Reactors**

<b>Reactor</b>	<b>Target Residual DO Concentration, mg O<sub>2</sub>/L</b>
BIOPHO-PX1	0.8 ± 0.1
BIOPHO-PX2	1.5 ± 0.1
BIOPHO-PX3	0.8 ± 0.1
BIOPHO-PX4	1.5 ± 0.1

**Table 3: Phase Length per Cycle**

	<b>BIOPHO-PX 1 and 2</b>	<b>BIOPHO-PX 3 and 4</b>
Anaerobic, hrs	1.0	1.0
Aerobic, hrs	1.5	2.0
Anoxic, hrs	3.0	2.5
Settling/Decant, hrs	0.5	0.5

The lengths of the aeration phase in each of the experimental reactors were not controlled by online monitoring. Instead, each reactor had a pre-set aeration length, and air was supplied by aquarium pumps through bubble diffusers located 1-in from the bottom of the reactors.

Online DO control for each reactor was achieved using a Hach LDO probe to measure the DO concentration during the aerobic phase of the cycle; the DO signal was monitored continuously using a Hach SC-100 controller. The SC-100 was programmed with the acceptable range of DO concentration for each reactor (Table 2). The probe measured the DO concentration every 30 seconds. If the concentration reading was below the set range of concentrations the SC-100 would activate the aeration pumps, which would to aerate the reactors. Likewise, if the concentration was above the set range, the controller would deactivate the pumps until the DO concentration had decreased to within the acceptable range.

The impact of the SRT on the BIOPHO-PX process and nitrification was also evaluated in this study. The BIOPHO-PX configurations were operated at the setpoints listed in Table 2 at SRTs of 10 and 20 days. The reactors were allowed to stabilize over a period of approximately 3 SRTS before their performance was assessed at each SRT.

The substrate for these investigations was a mixture consisting of 10% VFA-rich fermenter liquor and 90% filtered municipal wastewater (by volume), to ensure a supply of

VFAs to the reactors to drive EBPR. The fermenter liquor was obtained by fermenting primary municipal solids from Pullman, WA WRRF, in a completely mixed fermenter fed on a mass basis and controlled at a 4-day SRT at ambient temperature, 20-26 °C. The fermenter liquor was regularly characterized over the course of these investigations for PO<sub>4</sub>-P, NH<sub>4</sub>-N, and VFA concentrations. The average concentrations for the fermenter effluent can be seen in Table 4. Note that the majority of the VFAs consisted of acetic acid and propionic acid, with the propionic acid concentration slightly lower than the acetic acid concentration. This near 50:50 ratio has been shown to enhance the biological system for PAOs over GAOs to aid in EBPR due to PAOs ability to easily uptake either substrate (Lopez-Vazquez, et al. 2009). Screened and de-gritted raw wastewater was obtained weekly from the Moscow, ID WRRF and stored at 4°C in polyethylene jugs until use. Wastewater was filtered through a fine mesh filter prior to daily batching of feed.

**Table 4: Primary Solids Fermenter Liquor Characteristics**

	<b>Concentrations, mg/L (n=18)</b>
PO <sub>4</sub> -P	27.3 ± 4.8
NH <sub>4</sub> -N	44.7 ± 22.7
Total VFAs	1349.2 ± 419.5
Acetic Acid	611.3 ± 213.8
Propionic Acid	502.4 ± 205.7

## Chapter 4: Methods

In order to characterize the performance of the biomass in each reactor, comprehensive wet chemistry assessments of bulk solution were performed. PO<sub>4</sub>-P, NH<sub>4</sub>-N, NO<sub>3</sub>-N, and NO<sub>2</sub>-N were monitored over an entire cycle as well as VFAs, PHA, and glycogen. Samples were also collected to monitor mixed-liquor suspended solids (MLSS) in the reactors.

For soluble constituents, samples were first centrifuged to remove solids/biomass and then filtered through a 0.22  $\mu$  m syringe filter (Millipore Corp., Billerica, MA, USA) prior to testing. PO<sub>4</sub>-P was determined in accordance with Hach (Loveland, CO, USA) method 8048 (method equivalent to Standard Methods 4500-PE (Clesceri, Greenberg and Eaton 1998)). Soluble NO<sub>3</sub>-N was determined in accordance with Hach method 10020. Soluble NH<sub>4</sub>-N testing followed Hach method 10031. Soluble NO<sub>2</sub>-N was determined using Hach method 8153 and method 8507. A Spectronic® 20 Genesys™ spectrophotometer (Thermo-Fisher Scientific Corp, Waltham, MA, USA) was utilized to measure the absorbance of the reacted sample at a wavelength of 890 nm for PO<sub>4</sub>-P, 410 nm for NO<sub>3</sub>-N, 507 nm for NO<sub>2</sub>-N and 655 nm for NH<sub>4</sub>-N. Phosphate, NO<sub>3</sub>, and NH<sub>3</sub> concentrations were determined utilizing a standard curve ( $R^2 > 0.99$ ) (Coats, Dobroth and Brinkman 2013).

MLSS was measured in accordance with Standard Methods 2540 D (Clesceri, Greenberg and Eaton 1998). Measurement of pH was accomplished with a Thermo-Fisher Scientific Accumet AP85 Waterproof pH/Conductivity Meter (Coats, Dobroth and Brinkman 2013).

VFAs (acetic, propionic, butyric, isobutyric, valeric, isovaleric, and caproic acids) and methanol were quantified using a Hewlett-Packard 6890 series gas chromatograph

(Agilent Technologies, Inc., Santa Clara, CA, USA) equipped with a flame-ionization detector and a Hewlett-Packard 7679 series injector. The system was interfaced with the Hewlett-Packard GC ChemStation software version A.06.01. VFA separation was achieved using a capillary column (Heliflex® AT™-AquaWax-DA, 30 m x 0.25 mm ID, W. R. Grace & Co., Deerfield, IL, USA) which was ramped from an initial 50°C to 200°C in three steps (following 2 min at 50°C, ramp to 95°C at 30°C min<sup>-1</sup> then to 150°C at 10°C min<sup>-1</sup> and hold for 3 min; finally, ramp to 200°C at 25°C min<sup>-1</sup> and hold for 12 min) with helium as the carrier gas (1.2 mL min<sup>-1</sup>). The split/splitless injector and detector were operated isothermally at 210 and 300°C, respectively. Prior to analysis, samples were acidified to a pH of 2 using HCl. 0.5  $\mu$  L of each sample was injected in 20:1 split mode. VFA concentrations were determined through retention time matching with known standards (Sigma-Aldrich Co., St. Louis, MO, USA; Thermo Fisher Scientific Inc., Waltham, MA, USA) and linear standard curves ( $R^2 > 0.99$ ) (Coats, Dobroth and Brinkman 2013).

Biomass PHA content was determined by gas chromatography/mass spectrometry (GC-MS) as described in Coats et al. (2011). Total intracellular PHA content was determined on a percent dry weight cell basis (mass PHA (mass of biomass)<sup>-1</sup>, w/w) (Coats, Dobroth and Brinkman 2013).

In addition to monitoring the BIOPHO-PX process from a bulk parametric basis, qPCR analysis was used to quantify the populations of AOBs, NOBs, PAOs and GAOs in the system. qPCR is a useful tool for detecting specific groups of microorganisms present in activated sludge environments, and, when coupled with performance measurements, can provide critical information related to process operations and control. In qPCR analysis, a segment of 16S rDNA specific to the class of microorganism of interest is selected and then

amplified using DNA polymerase enzymes and short lengths of single-stranded DNA called primers which are specific to the gene of interest. The nucleic acids for amplification are removed by disrupting the cells and genetic material is purified prior to qPCR. As the amplification process proceeds, dye is complexed with DNA that fluoresces when it binds to double-strand DNA. The intensity of fluorescence corresponds to the relative quantity of the bacteria of interest compared to the total microorganism community (Metcalf and Eddy 2014, Fitzgerald, et al. 2015, Im, Jung and Bae 2014).

Quantitative real-time PCR (qPCR) was used to quantify 16S rDNA genes from total bacteria, *Accumulibacter* (the model PAO), and GAOs to provide an estimation of relative abundance. qPCR was conducted on a StepOne Plus™ Real-Time PCR system (Applied Biosystems, Foster City, CA) using iTaq™ SYBR® Green Supermix w/ROX (Bio-Rad Laboratories, Inc., Hercules, CA, USA) with a total reaction volume of 25 µl. Total bacterial and total *Accumulibacter* 16S rDNA genes were quantified with primer sets 341f/534r and 518f/846r, respectively GAOs were quantified using primer set GAOQ431f/GAOQ989r (specifically designed to target *Candidatus* *Competibacter phosphatis*, which is a putative model GAO and the total bacteria primer set. qPCR conditions were as follows: 3 min at 95°C, 45 cycles of 30 sec at 95°C, 45 sec at 60°C, and 30 sec at 72°C. All unknown samples were assessed in triplicate with 5 ng of total genomic DNA per reaction. Amplification efficiency was estimated for each primer set using baseline-corrected fluorescence data (from StepOne Software v2.0) with LinRegPCR. The cycle threshold was set at a constant value across all samples based on location within the log-linear region for determination of C<sub>q</sub> values (cycle number at which the measured fluorescence exceeds the cycle threshold). Gel

electrophoresis of qPCR products confirmed the presence of a single band for all GAO and PAO samples (Winkler, Coats and Brinkman 2011).

## Chapter 5: Results and Discussion

As described, four SBRs operated in the BIOPHO-PX mode were operated and evaluated for this research. Investigations were first conducted at a 10 day SRT. Reactors operations were then re-set to a 20 day SRT, and after a period of stabilization, the process was assessed. Results from this research are presented and discussed below.

### 5.1 10-Day SRT

Experimental reactors were operated at a 10-day SRT, at the set points given in Table 2, for a period of 97 days. The process was monitored for phosphorous and nitrogen removal as well as nitrification control. In addition, three complete comprehensive assessments were performed on BIOPHO-PX 3 and 4, where samples were taken approximately every 30 minutes from the beginning of an operational cycle. Performance results for all four reactors are discussed in the following sections. A summary of reactor phosphorous and ammonia removal over the 97-day period can be seen in Table 5. Figure 12 through Figure 15 show the concentrations of phosphorous and nitrogen species across an entire 6-hour operational cycle.

**Table 5: Summary of Average Concentrations for BIOPHO-PX 1 through 4 at 10-day SRT**

<b>n=6</b>	<b>Avg. Influent PO<sub>4</sub>-P (mg/L)</b>	<b>Anaerobic PO<sub>4</sub>-P Release (mg/L) n=3</b>	<b>Avg. Effluent PO<sub>4</sub>-P (mg/L)</b>	<b>Avg. Influent NH<sub>3</sub>-N (mg/L)</b>	<b>Avg. Effluent NH<sub>3</sub>-N (mg/L)</b>
BIOPHO-PX 1	3.1 ± 0.5	10.3 ± 1.3	0.7 ± 0.6	26.3 ± 8.0	26.7 ± 6.0
BIOPHO-PX 2	2.4 ± 0.3	12.1 ± 2.5	0.8 ± 0.5	25.4 ± 12.1	24.0 ± 7.2
BIOPHO-PX 3	6.4 ± 0.9	17.8 ± 0.4	0.6 ± 0.4	19.9 ± 7.2	1.2 ± 2.2
BIOPHO-PX 4	2.2 ± 0.3	18.1 ± 2.8	0.5 ± 0.5	13.1 ± 1.3	0.4 ± 0.8

### 5.1.1 Nitrogen Removal in Reactors with 10-day SRT

Ultimately, the reactors identified as BIOPHO-PX 1 and 2 were not able to achieve nitrogen removal at the 10 day SRT. Table 5 shows that the influent and effluent  $\text{NH}_4\text{-N}$  concentrations were essentially unchanged over an operational cycle for both reactors, with BIOPHO-PX2 having a slight decrease in ammonia. Figure 12 and Figure 13, show nearly straight lines for ammonia concentration across the length of the cycle, indicating little to no nitrogen removal. Total Nitrogen Removal is calculated as the difference between influent and effluent nitrogen species concentrations BIOPHO-PX 1 had a calculated average total nitrogen removal (TNR) value of  $11.9\% \pm 8.8\%$  (Table 6). BIOPHO-PX 2 had a slightly higher TNR at  $22.5\% \pm 1.5\%$  (Table 6). These values are very low for a typical BNR removal system, which would normally produce values closer to 90-92% (Tian, et al. 2011, J. Im, et al. 2014, Liu, et al. 2013). The lack of ammonia oxidation/nitrification most likely stems from the fact the fact that BIOPHO-PX 1 and 2 were operated at the shortest aeration time; in combination with the relatively short SRT and, for BIOPHO-PX 1, low residual DO, it would appear that the AOB population was not able to establish in the reactors. The aerobic SRT, which is the critical fraction of the total SRT related to nitrification (which is an obligate aerobic process) was 3.3 days, and further likely contributed to nitrification inhibition; nitrification at the temperature maintained in these lab-based operations (20-26°C) and the associated low aeration conditions would typically not be expected to commence until aerobic SRT was increased to 3 days (Grady Jr, et al. 2011).

Regarding the microbial populations, the relative populations of microorganisms in the reactor can be seen in Table 7. The AOB populations for BIOPHO-PX 1 and 2 are 0.03% and 0.04%, respectively (note that these percentages reflect the fraction of the total microbial

population). This population is too small to effectively oxidize the influent ammonia. The lack of AOB growth coupled with the short SRT and aeration length are reflected in the MLSS concentrations shown in Table 8, with BIOPHO-PX1 having the lowest concentration and BIOPHO-PX 2 having the second lowest. The biomass was not able to properly grow to concentrations in the 3000 - 4000 mg/L range that one would typically see in a BNR facility (Oehman, Yuan, et al. 2005, Winkler, Coats and Brinkman 2011).

Another reason the AOB population could be hindered in BIOPHO-PX 1 and 2 is the competition for the DO in system with PAOs. PAOs are able to uptake oxygen faster than AOBs due to the size and effectiveness of heterotrophs compared to autotrophs (Zeng, Yang, et al. 2011). As described, to control the process at nitritation, in these systems there was purposefully a limited amount of dissolved oxygen; with PAOs using oxygen first, there was likely very little residual DO for the AOBs to utilize for growth, maintenance, and ammonia oxidation. PAO populations for BIOPHO-PX 1 and 2 are 30.6% and 9.8%, respectively. Considering the low AOB populations and the fact that PAOs were removing  $\text{PO}_4\text{-P}$  further confirms that PAOs are able to use the oxygen in the system before AOBs are able to utilize it and therefore grow and perform other cellular functions (P-removal). This is also most likely why in all of the reactors PAO populations are larger than the AOB populations.

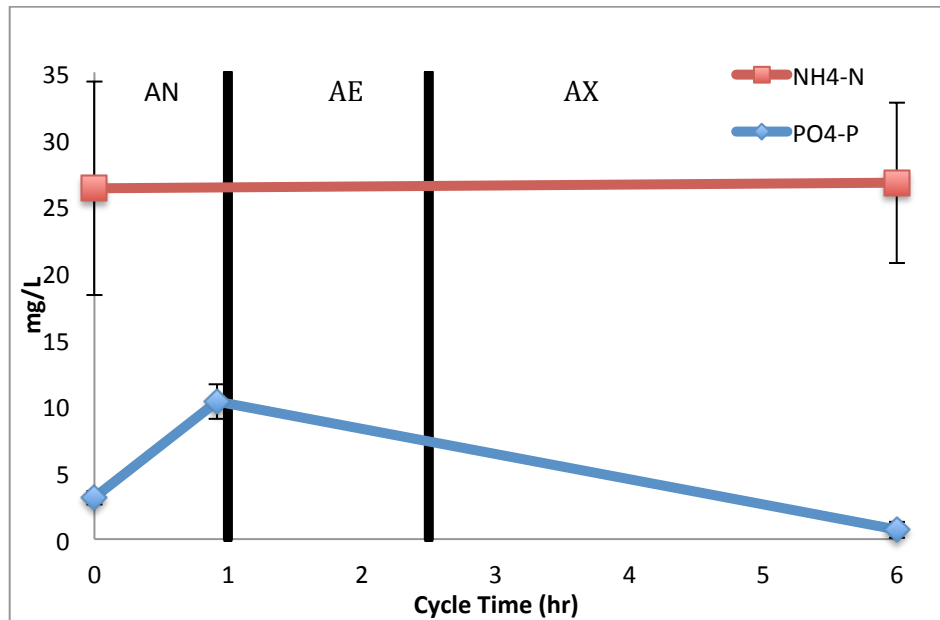


Figure 12: Average BIOPHO-PX1 at 10 day SRT n=3.

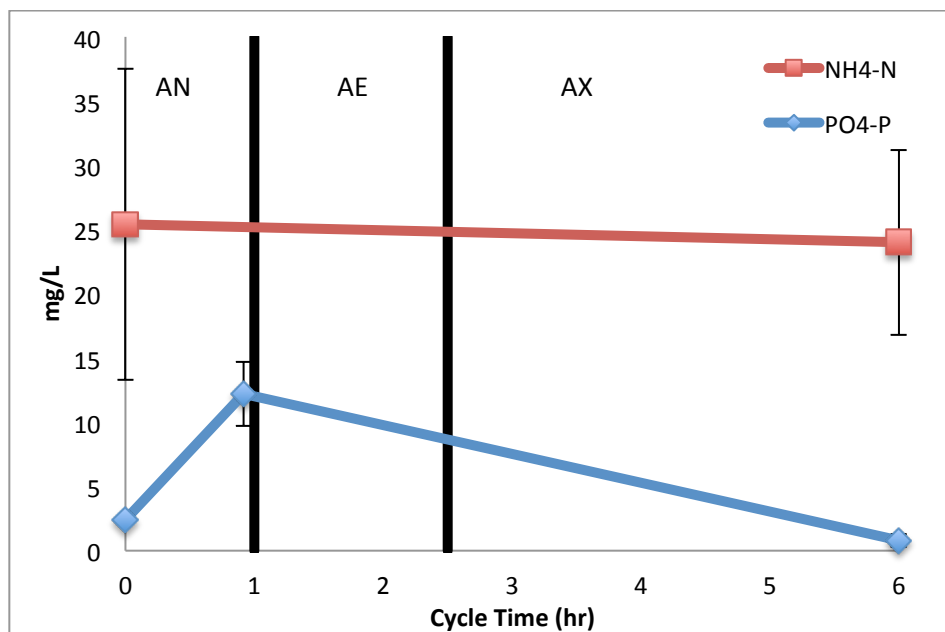


Figure 13: Average BIOPHO-PX 2 at 10 day SRT n=3

In contrast to BIOPHO-PX reactors 1 and 2, the MLSS enriched in BIOPHO-PX 3 was able to perform nitrogen removal (Table 5, Figure 14a-d). The TNR for BIOPHO-PX 3 was calculated to be  $86.3\% \pm 17.7\%$ . This is the highest TNR of all the reactors with a 10-

day SRT and closest to the typical TNR range in BNR systems: 90-92% (Tian, et al. 2011, J. Im, et al. 2014, Liu, et al. 2013). It would appear that the 33% increase in aerobic SRT (from 2.5 to 3.33 days) was sufficient to yield a critical mass of autotrophs, even though the residual DO was maintained quite low (compared with conventional nitrification practices). BIOPHO-PX 3 also had the highest  $\text{NO}_2\text{-N}$  accumulation at  $49.3\% \pm 12\%$ .  $\text{NO}_2\text{-N}$  accumulation was calculated as the percentage of ammonia oxidized (or  $\text{NO}_x$  produced) that is nitrite, with the remainder represented as nitrate (Lemaire, Marcelino and Yuan 2008). Therefore for this reactor, at the end of the aerobic period essentially 50% of the  $\text{NH}_4\text{-N}$  that had been oxidized is  $\text{NO}_2\text{-N}$  and the other 50% is  $\text{NO}_3\text{-N}$  (on average). For a system optimized for nitrification,  $\text{NO}_2\text{-N}$  accumulation values would typically be 81-100% (Lemaire, Marcelino and Yuan 2008, Guo, et al. 2008, J. Im, et al. 2014, W. Zeng, Y. Zhang, et al. 2010, W. Zeng, et al. 2009).

Examining the nitrogen cycling further, as shown in Figure 14a-d, it was observed that after ammonia oxidation begins there is a lag in nitrite oxidation to nitrate. The observed lag in nitrite oxidation likely was driven by the low residual dissolved oxygen concentration. This lag along with the  $\text{NO}_2\text{-N}$  accumulation suggests that the system could be further optimized towards nitrification. Regarding the microbiology, the AOB population in BIOPHO-PX 3 is still small compared to the other microorganisms at 0.2% but it is sufficiently large enough to oxidize the influent  $\text{NH}_4\text{-N}$  to an average effluent value of 1.2 mg/L. Interestingly, the NOB population persists in the system at 0.5%, even at a low residual DO and in greater numbers than the AOB population. If further wash out of the NOBs could be achieved, the system would continue towards optimization of nitrification.

As a final contrast, the MLSS in BIOPHO-PX 4 performed better than observed in BIOPHO-PX 1 and 2, yet not quite as well as BIOPHO-PX 3. The TNR for BIOPHO-PX 4 was calculated to be  $52.9\% \pm 14.6\%$  and  $\text{NO}_2\text{-N}$  accumulation at  $30.4 \pm 44.2$ . It is quite interesting that, despite the same aerobic SRT as BIOPHO-PX 3 (3.33 days) and an increased residual DO, less nitrogen removal was realized. BIOPHO-PX 4 also shows a nitrate lag in the aerobic period where first ammonia is oxidized completely to  $\text{NO}_2\text{-N}$  and then to  $\text{NO}_3\text{-N}$  (Figure 15a-d); the lag, however, was not as pronounced as observed in BIOPHO-PX 3. This indicates that if the aeration period would have been stopped when the ammonia was completely oxidized to  $\text{NO}_2\text{-N}$ , additional  $\text{NO}_2\text{-N}$  accumulation could have possibly been realized. The NOB population in BIOPHO-PX 4 is the highest of all four reactors, which aligns with the less pronounced lag in nitrite oxidation. This is most likely due to the fact that, among all four reactor configurations evaluated, BIOPHO-PX 4 had the highest residual DO as well as the longest aeration length. This reactor also has the largest AOB population at 0.6% (Table 7). Other studies have shown similar results using qPCR analysis with an AOB concentration as low as 0.55% of the population in a reactor and ammonia oxidation occurring (Fitzgerald, et al. 2015). However, this large AOB population did not allow for the largest TNR. This TNR value is most likely due to lack of carbon in the anoxic period to allow for total denitrification therefore resulting in a larger TNR.

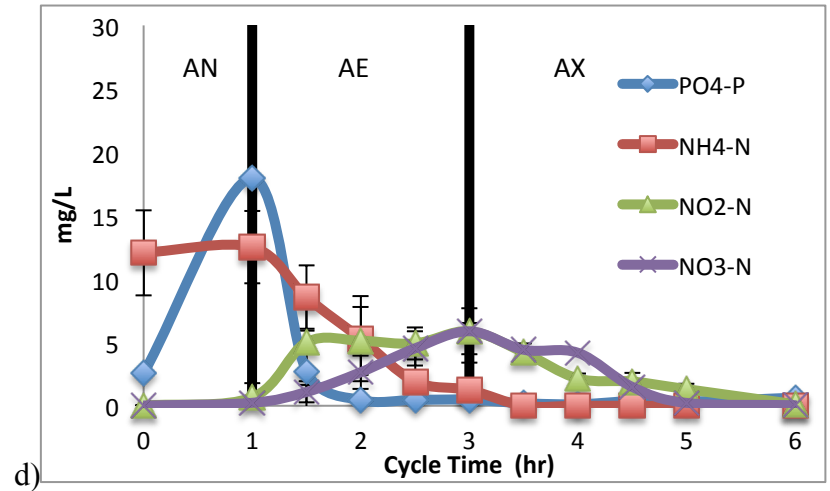
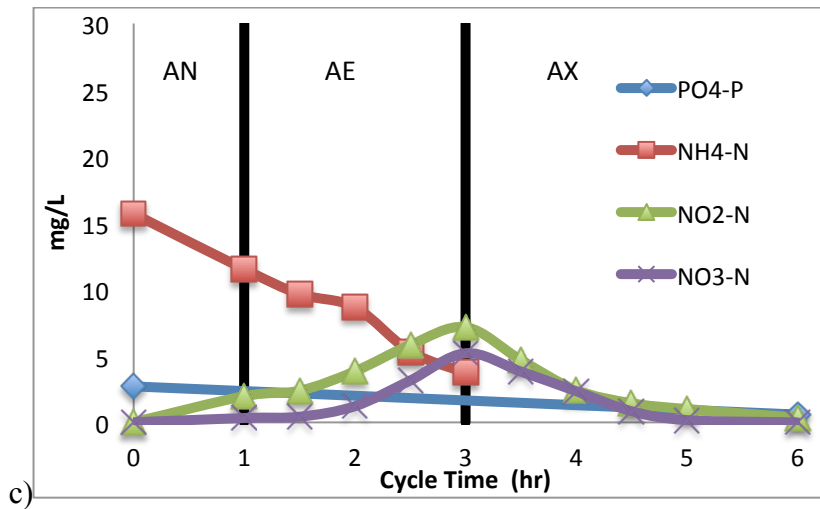
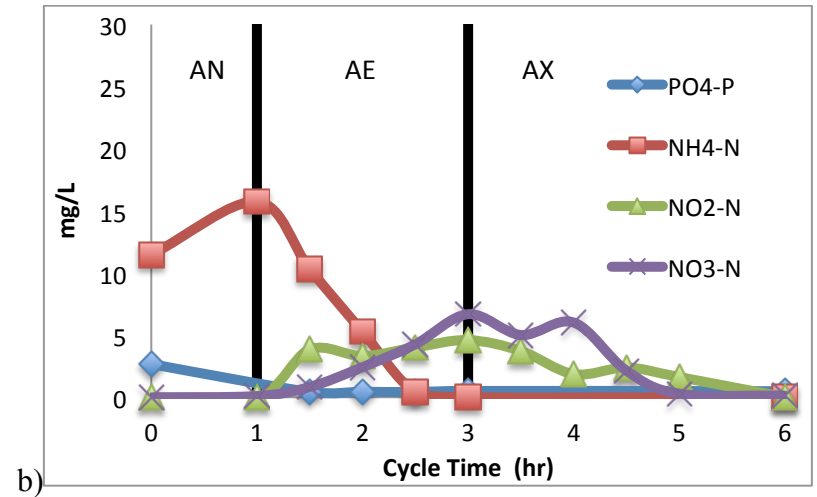
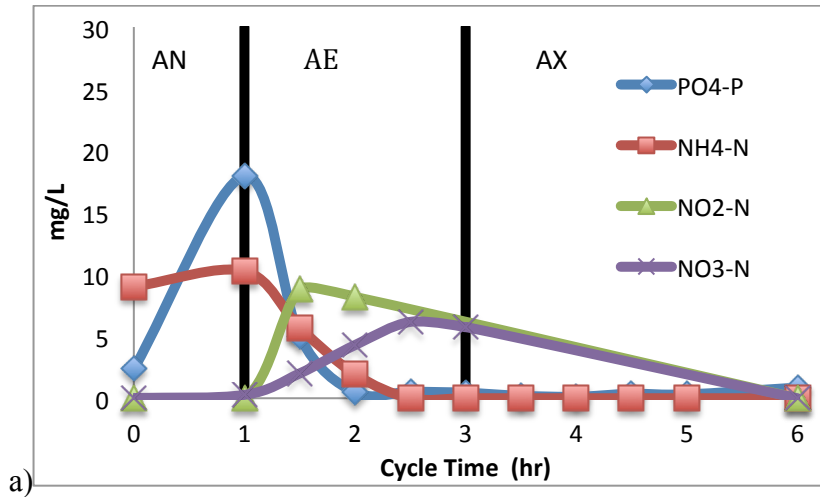


Figure 14: BIOPHO-PX 3 on a)10/1/14, b)10/9/14 and c)10/15/14, and d)Average BIOPHO-PX 3 Phosphorous and Nitrogen across the cycle n=3

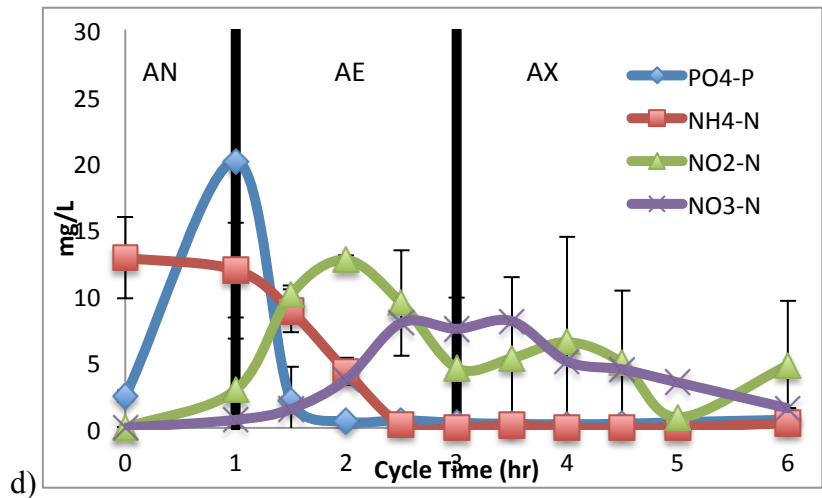
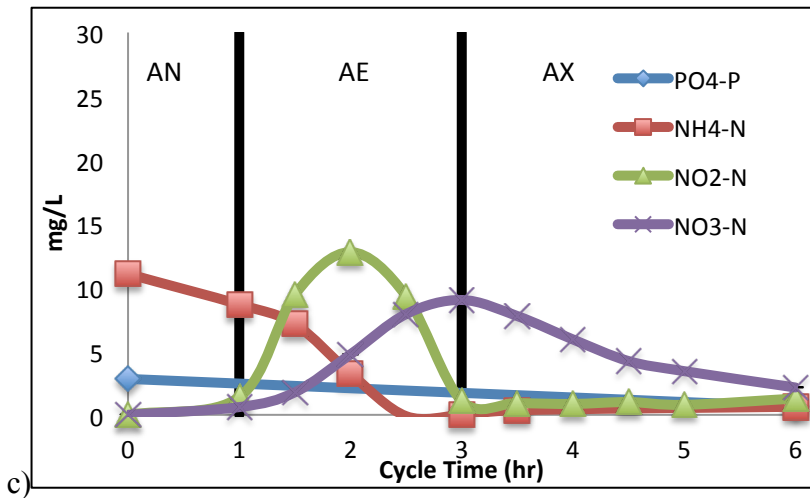
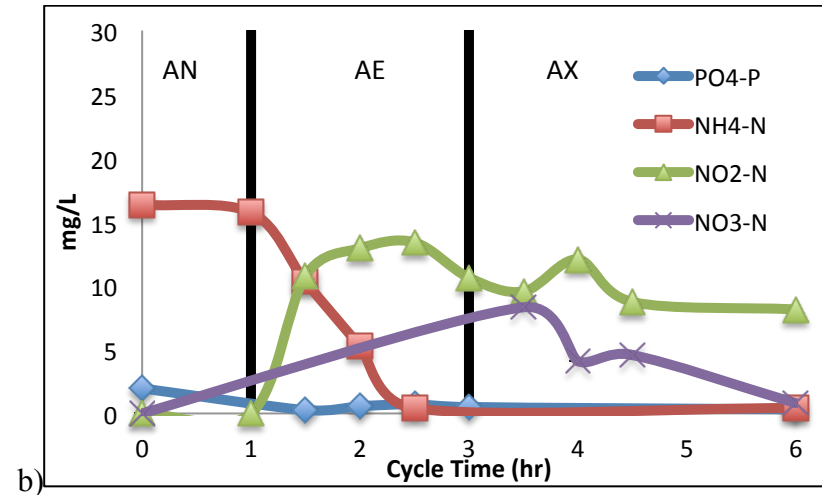
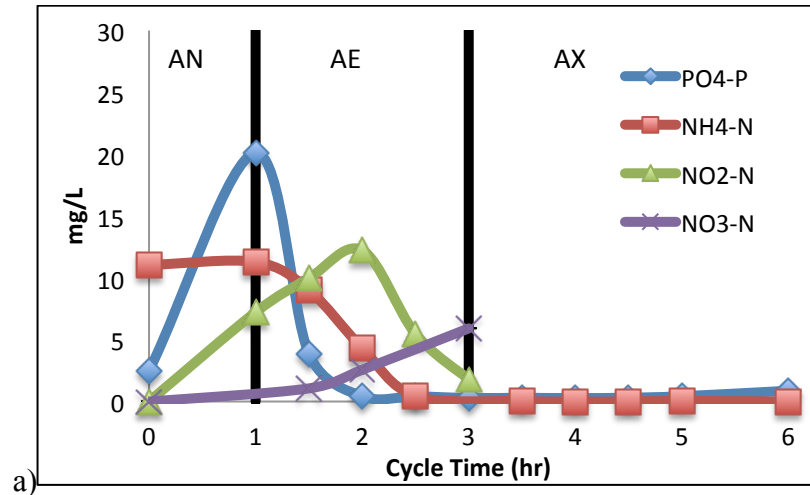


Figure 15: BIOPHO-PX 4 on a) 10/1/14, b) 10/9/14 and c) 10/15/14, and d) Average BIOPHO-PX 4 Phosphorous and Nitrogen across the cycle n=3

**Table 6: Percent Removal for BIOPHO-PX Reactors at 10-day SRT**

<b>Reactor</b>	<b>TPR (%)</b>	<b>TNR(%)</b>	<b>NO<sub>2</sub>-N Accum. (end AE) (%)</b>
BIOPHO-PX 1	85.2 ± 1.6	11.9 ± 8.8	-
BIOPHO-PX 2	84.8 ± 10.8	22.5 ± 1.5	-
BIOPHO-PX 3	85.1 ± 8.9	86.3 ± 17.7	49.3 ± 12
BIOPHO-PX 4	85.4 ± 9.5	52.9 ± 14.6	30.4 ± 44.2

**Table 7: qPCR analysis for 10-day SRT**

	<b>% PAOs</b>	<b>%GAO</b>	<b>% AOBs</b>	<b>% NOBs</b>	<b>NOB/AOB</b>
BIOPHO-PX 1	30.6	1.2	0.03	2.9	95.0
BIOPHO-PX 2	9.8	0.4	0.04	1.8	43.8
BIOPHO-PX 3	4.5	0.05	0.2	0.5	3.2
BIOPHO-PX 4	40.0	0.6	0.6	11.4	18.1

### 5.1.2 Phosphorous Removal in Reactors with 10-day SRT

All four of the BIOPHO-PX reactors were able to achieve phosphorous removal, albeit not to typically low concentrations that can be achieved via EBPR (which can be as low as 0.14 mg/L (Winkler, Coats and Brinkman 2011)). Table 5 shows the average influent and effluent PO<sub>4</sub>-P for the reactors, as well as the end anaerobic concentration. MLSS on both of the reactors exhibited a typical EBPR release of P in the anaerobic environment, before removing excess P to less than 1 mg/L on average. Total phosphorous removal (TPR) for BIOPHO-PX 1 through 4 are on average 85.2%, 84.8%, 85.1% and 85.4%, respectively (Table 6). These are slightly lower than typical EBPR TPR values, which normally range from 97-99% (Liu, et al. 2013, Tian, et al. 2011). The average influent VFA-to-P ratios can be seen in Table 9; these ratios were in the expected range for EBPR removal (Winkler,

Coats and Brinkman 2011). While this stoichiometric ratio would suggest that better overall P removal should occur, there are two potential reasons that the reactors were not producing effluent with lower PO<sub>4</sub>-P concentrations (97-99% TPR (Liu, et al. 2013, Tian, et al. 2011)). One reason is that the GAOs in the system were consuming some of the influent VFAs, ultimately reducing the total amount available for PAOs to synthesize PHA and perform P removal; as shown, there were GAOs present in the system (Table 7). The second reason may be due to the low residual DO concentration relative to typical EBPR systems (with a residual DO concentration of 2.0 mg/L). Ultimately, the microorganisms were in constant competition for the small amount of oxygen, which could have affected aerobic bioenergetics (i.e., ATP synthesis via oxidative phosphorylation) required for excess P removal.

Considering expected EBPR behavior, the observed anaerobic P release indicates that the PAOs in the system removed VFAs during the anaerobic phase to produce PHA stores. The P/C ratio is the measurement of phosphorous released in the anaerobic zone and the VFAs in the influent. This ratio is important for assessing whether or not the system has sufficient VFAs to remove the phosphorous. The P/C ratios were generally consistent with those observed in previous BIOPHO-PX research (Figure 11, (Winkler, Coats and Brinkman 2011)). Moreover, the P/C ratios were generally consistent with PAO-enriched cultures capable of performing EBPR ranging from 0.17-0.5 (Winkler, Coats and Brinkman 2011, Oehman, Yuan, et al. 2005, Taya, et al. 2013, Carvalheira, et al. 2014, Liu, et al. 2013). However, the BIOPHO-PX P/C values (Table 9) were on the lower end of the typical range. Nevertheless, all four reactors were enriched for PAOs over GAOs, which further indicates the ability of PAOs to thrive at low DO (Carvalheira, et al. 2014).

**Table 8: Average MLSS concentrations for BIOPHO reactors at a 10 day SRT n=3**

<b>Reactor</b>	<b>Average MLSS concentration (mg/L)</b>
BIOPHO-PX 1	1690 ± 246
BIOPHO-PX 2	1980 ± 442
BIOPHO-PX 3	2727 ± 428
BIOPHO-PX 4	3180 ± 610

**Table 9: Ratio of Influent VFAs to P and Effluent P**

<b>n=2, 2, 3, 3</b>	<b>Influent VFA: Influent P (C mmol/Pmmol)</b>	<b>AN P release:VFA (P mmol/ C mmol)</b>	<b>Effluent P mg/L</b>
BIOPHO-PX 1	22.3 ± 3.3	0.12 ± 0.01	0.7 ± 0.6
BIOPHO-PX 2	34.9 ± 14.8	0.19 ± 0.04	0.8 ± 0.5
BIOPHO-PX 3	28.1 ± 5.3	0.20 ± 0.06	0.6 ± 0.4
BIOPHO-PX 4	29.2 ± 3.9	0.24 ± 0.07	0.5 ± 0.5

### 5.1.3 DO Analysis for reactors at 10-day SRT

As described, this research employed the length of the aeration period and the DO setpoints to control for nitrification. A typical DO curve over the aeration period for the reactors can be seen in Figure 16, with average values seen in Table 10. Note that for approximately the first hour the DO concentration did not reach the target residual DO concentration setpoint, indicating that the organisms were utilizing most, if not all, DO as it enters the system. For BIOPHO-PX 4, when the system reached the residual DO setpoint (on average), the phosphorous had been removed, the nitrite concentration had reached its peak, and after this point nitrate began to form, indicating a possible opportunity to control for nitrification by adjusting the DO control in real-time. The variable (up and down) pattern observed in the DO curve, once the residual concentration has been reached is a common pattern seen in DO curves (Lemaire, Marcelino and Yuan 2008, Regmi, et al. 2014).

For BIOPHO-PX1 and 3, targeted for the low DO setpoint of 0.7 mg/L, the actual average residual DO is slightly above the target concentration (Table 10). For BIOPHO-PX 2 and 4 (the higher target residual DO concentration), the average residual DO concentration was slightly lower than the target concentration of 1.5 mg/L. All four reactors had, on average, a 30 minute lag time or longer, meaning that the system was not at its residual DO concentration for approximately the first 30 minutes of the aerobic phase.

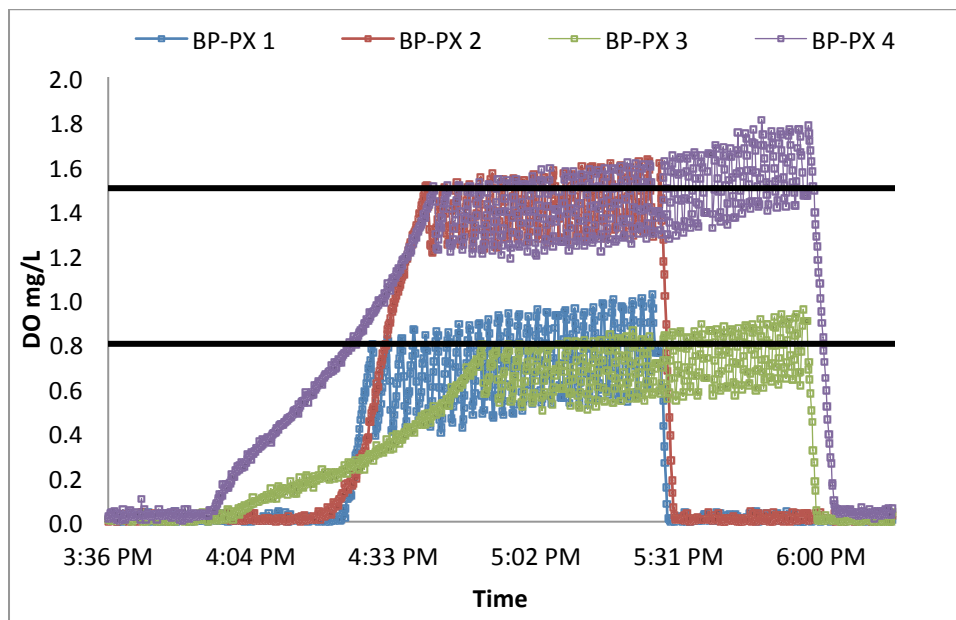


Figure 16: Typical DO Profiles for BIOPHO-PX 1 through 4 at 10-day SRT, 10/16/2014

Table 10: Average Residual DO concentrations over an aeration cycle and Aeration Length at the residual DO

n=6	BIOPHO –PX 1	BIOPHO –PX 2	BIOPHO –PX 3	BIOPHO –PX 4
Avg. Residual DO (mg/L)	0.73 ± 0.03	1.42 ± 0.03	0.73 ± 0.04	1.47 ± 0.05
Time at Residual DO (min)	63 ± 7	49 ± 14	75 ± 8	93 ± 18

### 5.1.4 10-day SRT Specific Rates

Table 11 shows the specific rates of phosphorus (P) release, phosphorus removal, ammonia oxidization and denitrification (SDNR) for the BIOPHO-PX reactors. N-species rates were not calculated for BIOPHO-PX 1 and 2 due to their insufficient nitrogen removal. Specific rates are calculated by normalizing the concentration of the species of interest during a specific time interval by dividing by the MLSS concentration. The TP values are very similar for all four reactors, which is reflected by the similar P release rates for all four reactors. BIOPHO-PX 3 had the highest TNR and percentage of nitrite accumulation, which is expected because it also has the highest rate of ammonia oxidation. These SNDR values are highest than expected if the carbon used for denitrification was simply endogenous decay and also higher than previous SNDRs using this post-anoxic configuration, suggesting a larger carbon savings in the microorganisms (Metcalf and Eddy 2014, Winkler, Coats and Brinkman 2011).

Table 11: 10-day SRT specific rates

n=1 or 3	P Release AN (mg P/ gVSS*hr)	P Removed AE (mg P/ gVSS*hr)	NH4 Oxidized (mg N/ g VSS *hr)	SDNR (mg NO <sub>x</sub> - N/gVSS*hr)
BIOPHO-PX 1	5.0 ± 1.1	4.9	-	-
BIOPHO-PX 2	5.1 ± 1.1	6.6	-	-
BIOPHO-PX 3	5.70	4.75	3.33 ± 0.29	1.42 ± 0.07
BIOPHO-PX 4	5.55	3.11	1.95 ± 0.49	1.67± 0.7

### 5.1.5 Summary and Conclusions for Reactors at 10-day SRT

In summary, operating at a 10 day SRT the operational conditions for BIOPHO-PX 1 and 2 were not capable of achieving nitrogen removal and therefore are not candidate

operational criteria for the BIOPHO-PX process. BIOPHO-PX 3 and 4 may be able to be optimized for nitrification and improving phosphorous removal utilizing further DO control investigations as well as carbon (PHA and glycogen) across the cycle, with BIOPHO-PX 4 showing the most promise with the nitrate lag.

## 5.2 20-Day SRT

As described, SRT was also an operational parameter evaluated for nitrification control. Thus, in addition to the 10 day SRT evaluation, the BIOPHO-PX SBRs were also operated and evaluated at a 20 day SRT (for a period of 160 days thus far), with the same set points as indicated in Table 2 and Table 3 for DO and aeration length. The same constituents were measured as the 10-day SRT. A summary of reactor phosphorous and ammonia removal over the 160-day period can be seen in Table 12. Figure 17 through Figure 20 show the concentrations of phosphorous and nitrogen species across an entire 6-hour operational cycle. A second aquarium pump was also added to each reactor to decrease the lag time before the target residual DO concentration was met.

Table 12: Average Phosphorous and Ammonia Concentrations at 20-day SRT

<b>n=3</b>	<b>Avg. Influent PO<sub>4</sub>-P (mg/L)</b>	<b>Anaerobic PO<sub>4</sub>-P Release (mg/L)</b>	<b>Avg. Effluent PO<sub>4</sub>-P (mg/L)</b>	<b>Avg. Influent NH<sub>3</sub>-N (mg/L)</b>	<b>Avg. Effluent NH<sub>3</sub>-N (mg/L)</b>
BIOPHO-PX 1	3.2 ± 0.3	17.1 ± 5.5	0.6 ± 0.4	21.6 ± 4.6	17.1 ± 5.1
BIOPHO-PX 2	2.9 ± 0.7	17.8 ± 4.1	0.5 ± 0.2	10.3 ± 1.8	0.4 ± 0.6
BIOPHO-PX 3	2.8 ± 0.6	16.0 ± 3.5	0.4 ± 0.2	10.2 ± 1.8	0.1 ± 0.2
BIOPHO-PX 4	2.6 ± 0.4	16.5 ± 4.1	0.3 ± 0.2	10.4 ± 1.9	0.1 ± 0.1

### 5.2.1 Nitrogen Removal in Reactors with 20-day SRT

As was observed at the 10 day SRT, BIOPHO-PX 1 was not able to achieve significant ammonia oxidation. While the AOB concentration in the system did increase from 0.03% (10-day SRT) to 0.3% (20-day SRT), the additional AOB population was insufficient to achieve much ammonia oxidation under the applied operating conditions. The increase in AOBs did allow for partial ammonia oxidation, the majority of which remained in the aerobic system as nitrite (see Figure 17a-d ). Consequently, the MLSS in BIOPHO-PX 1 only achieved TNR of 16%, with  $\text{NO}_2\text{-N}$  accumulation at 64%. While these results were an improvement from the reactor operating with a 10-day SRT, the results were far from optimal. BIOPHO-PX1 also has the lowest AOB population and lowest MLSS out of the four reactors (Table 15), further indicating that at the low residual DO setpoint and short aeration length there is simply not enough oxygen for the system to perform nitrogen removal (Zeng, Yang, et al. 2011).

In contrast to the MLSS in BIOPHO-PX 1, the biomass in reactors BIOPHO-PX 2, 3 and 4 were able to achieve ammonia oxidation. The amount of AOBs in BIOPHO-PX reactors increased (relative to the reactors with 10-day SRTs), confirming that an increase in the SRT does allow for an increase in AOB growth (consistent in all the reactors). The TNR for BIOPHO-PX 2, 3 and 4 was 81.9%, 79.3%, and 49.1%, respectively (Table 13). These values are low for a typical BNR removal system, which would normally have TNR values closer to 90-92% (Tian, et al. 2011, J. Im, et al. 2014, Liu, et al. 2013). BIOPHO-PX 2 had the highest average TNR (81.9%) and one of the highest average  $\text{NO}_2\text{-N}$  accumulations (40.4%); it also had the highest average AOB population, at 0.7%, of any of the reactors at both SRTs, indicating its potential to be further optimized to select for nitrification. Figure 13a-

d indicates that there is possible a slight lag of nitrification before nitrification begins that could be further exaggerated to control for nitrification.

Similar to BIOPHO-PX 2, BIOPHO-PX 3 and 4 were also able to remove nitrogen from the wastewater, however not as effectively. As shown in Figure 19a-d and Figure 20a-d, the two reactors ultimately were over-aerated, with nitrification occurring throughout the entire aerobic phase. As a further indication that nitrification control was not sufficient, nitrate began to form as soon as the aerobic phase began. This nitrification seen in the reactors is most likely caused by the second aquarium pump that was added to the system in order to reduce the lag time until the system reached its setpoint for residual DO (discussed below). The increase in oxygen supplied to the reactors also corresponds in an increase in NOB population in both reactors, which would also increase the nitrate formed.

An important part of nitrogen is the denitrification/denitrification that occurs in the anoxic environment. This environment allows for the reduction of the nitrogen species to nitrogen gas so that it can leave the activated sludge system. BIOPHO-PX 2 was able to totally remove nitrogen from the system through anoxic nitrite/nitrate reduction; this indicates that there was sufficient internal carbon stores available to the heterotrophs (PAOs and Ordinary Heterotrophic Organisms (OHO)) so that the addition of external carbon was not needed. BIOPHO-PX 3 and 4 were not able to completely denitrify in the post-anoxic zone, indicating a lack of sufficient internal carbon stores or possibly the incorrect form of internal carbon. Regarding organic carbon stores, Figure 21 and Figure 22 show the percent of PHA in the biomass as well as the concentration of VFAs and glycogen over the course of an operational cycle. As expected (per EBPR theory), the maximum PHA is accumulated during the first hour of the cycle (during the anaerobic period) as the VFAs are consumed.

After this first hour, PHA begins to decrease in the system, as aeration is turned on, again consistent with EBPR theory and reflecting that the MLSS is functioning in a respirative environment. The PHA is then essentially zero by the end of the aerobic period. This means that the nitrite/nitrate reduction is occurring by the microorganisms using their intracellular glycogen and that PAOs or GAOs could be responsible (Winkler, Coats and Brinkman 2011, Tsuneda, et al. 2006). The two subgroups of PAOs that have been identified are both capable of nitrite reduction, while only 1 of the 8 GAO subgroups is capable of nitrite reduction (Taya, et al. 2013); this is another reason PAOs should be enriched over GAOs in the BIOPHO-PX system. All four reactors have glycogen present throughout the cycle, but BIOPHO-PX 3 and 4 were not able to perform total denitrification. This indicates that perhaps there was not enough glycogen for the large MLSS concentration in those reactors or that it was not the proper form of carbon for the microorganisms to be able to use it for denitrification.

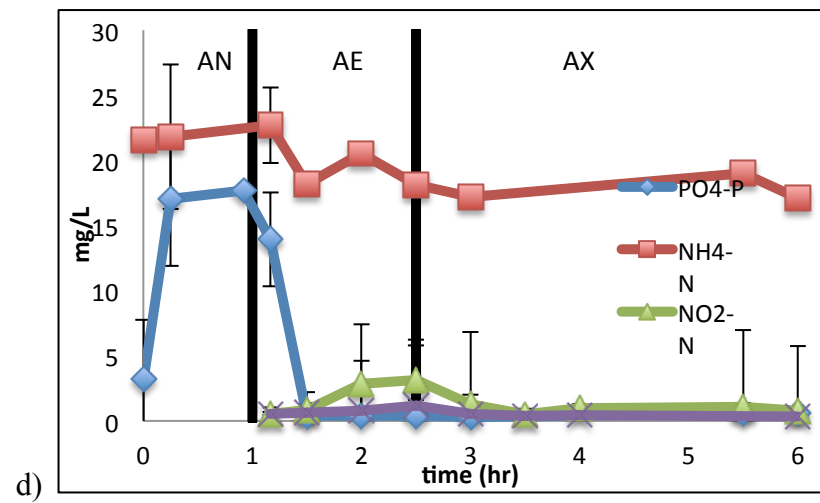
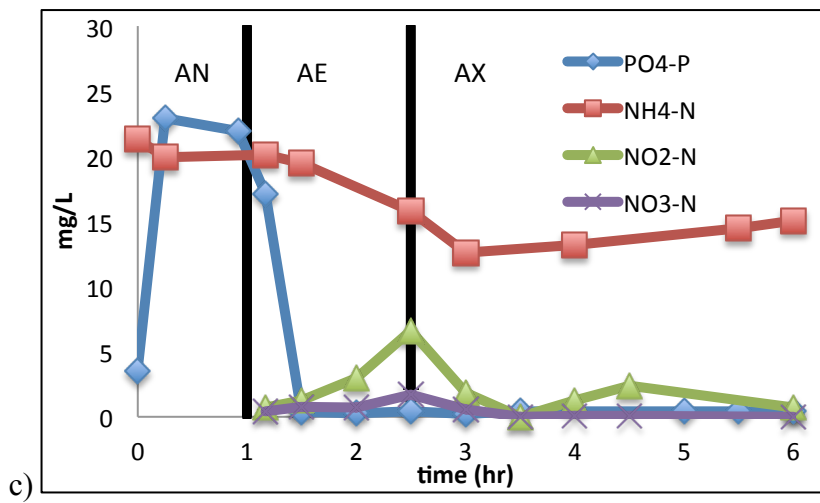
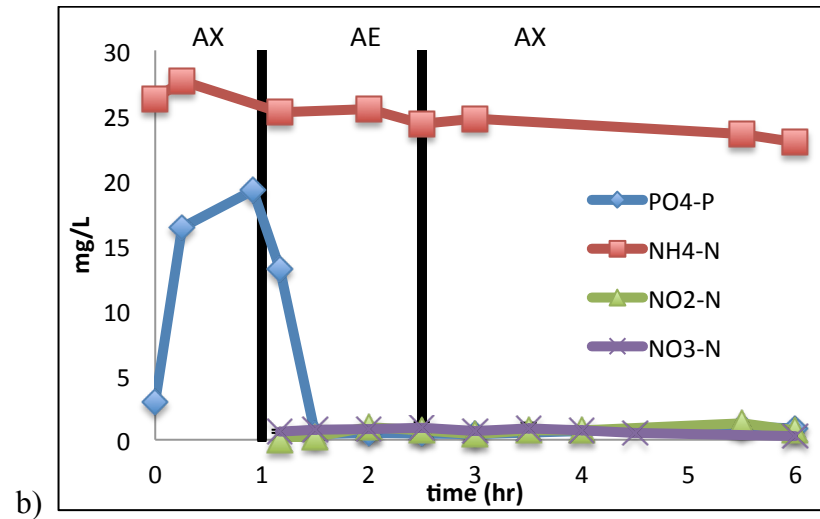
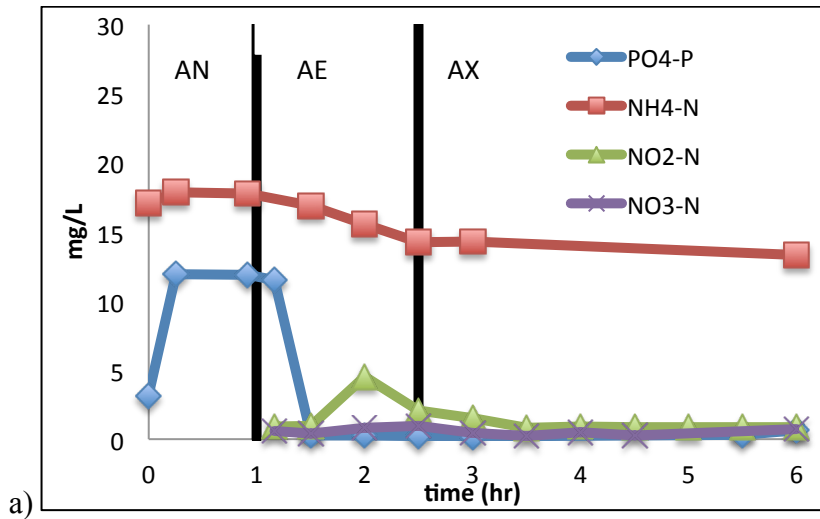


Figure 17: BIOPHO-PX 1 on a)2/16/15, b) 3/7/15 and c)3/16/15, and d)Average BIOPHO-PX 1 Phosphorous and Nitrogen across the cycle n=3

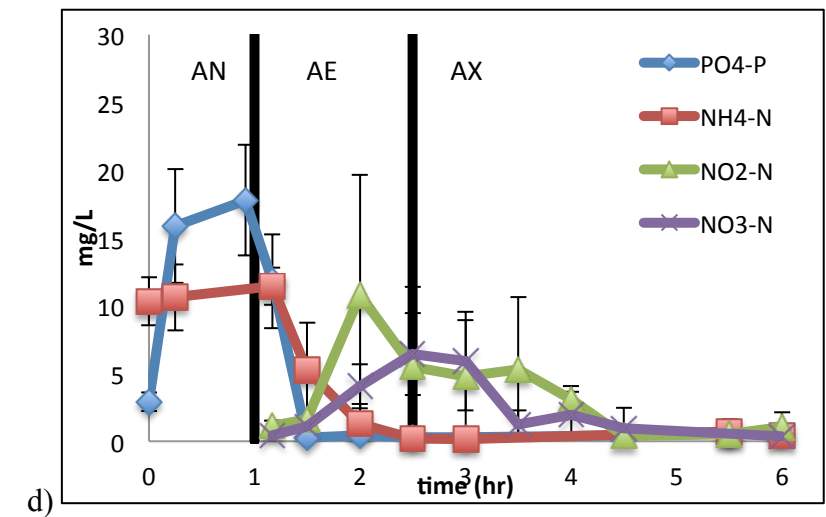
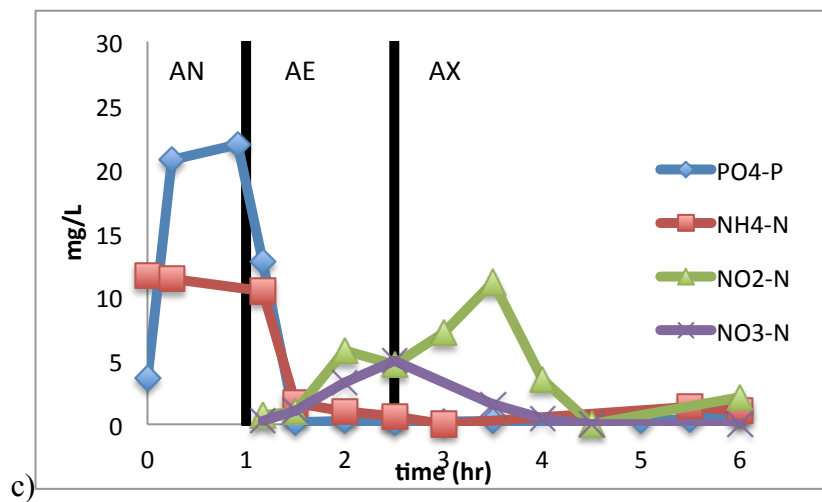
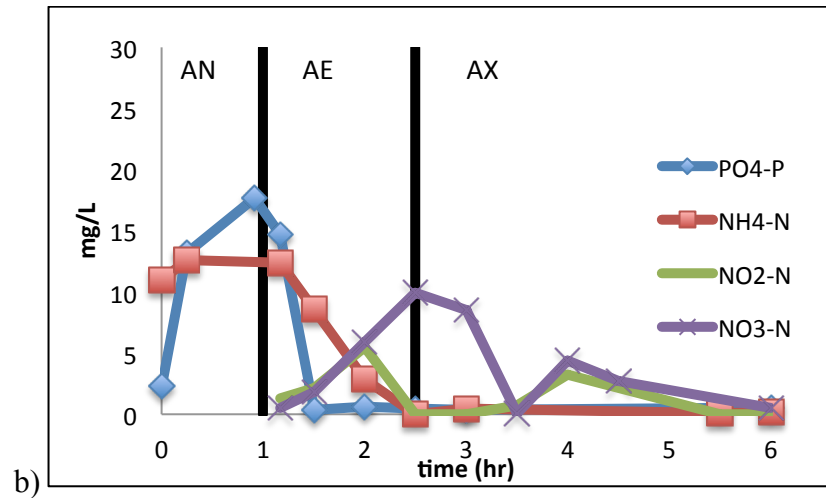
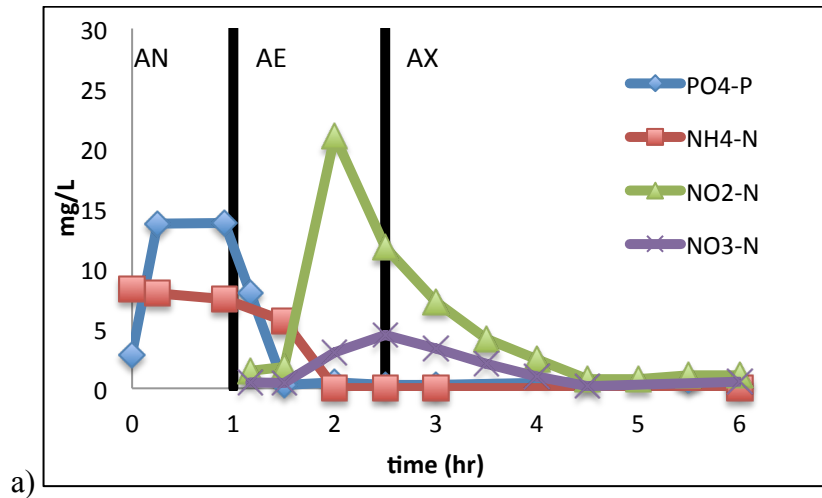


Figure 18: BIOPHO-PX 2 on a) 2/16/15, b) 3/7/15 and c) 3/16/15, and d) Average BIOPHO-PX 2 Phosphorous and Nitrogen across the cycle n=3

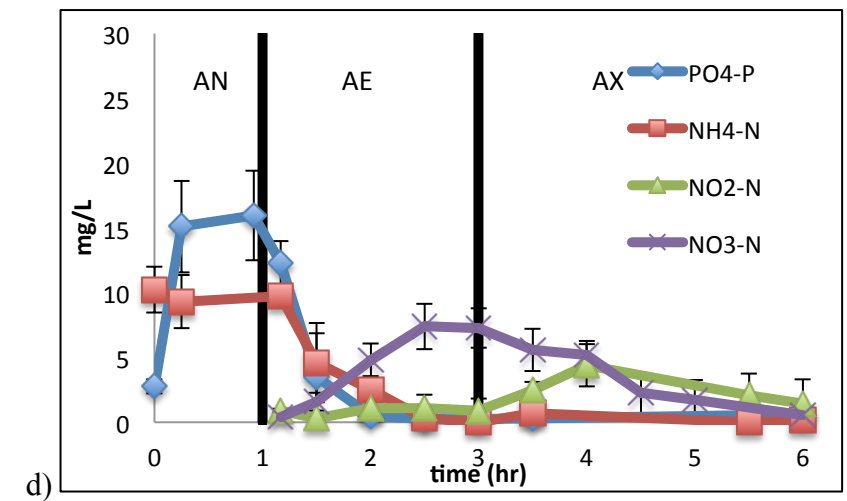
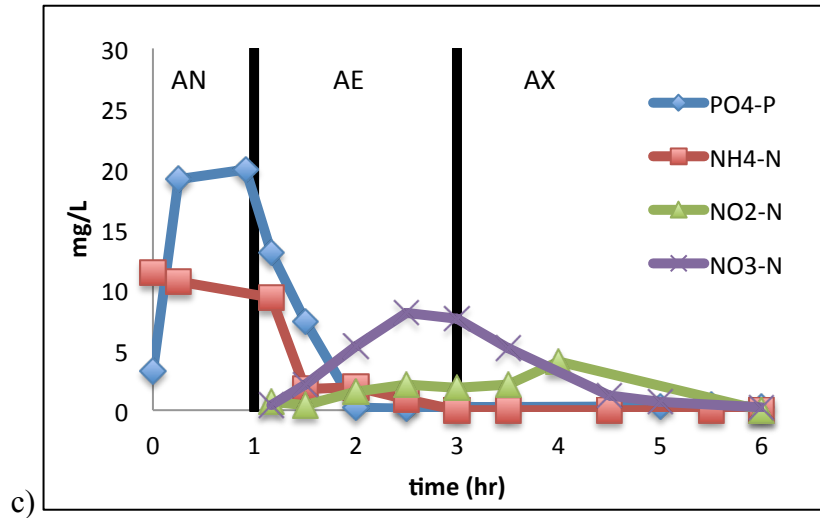
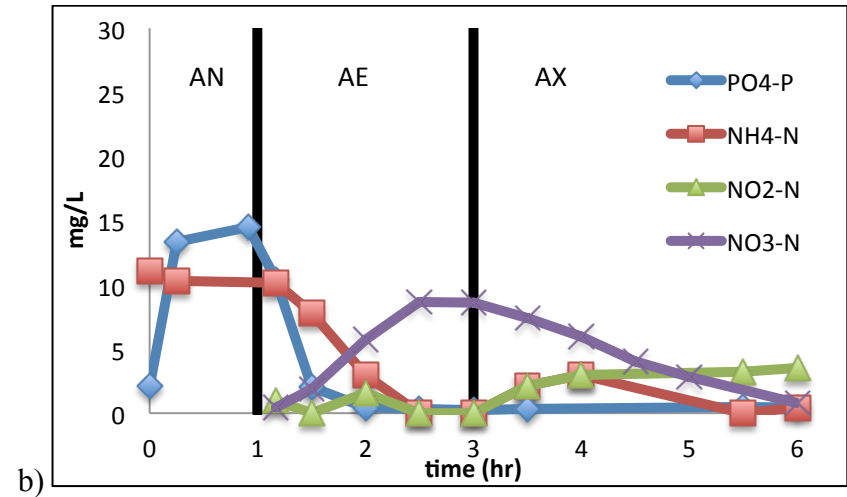
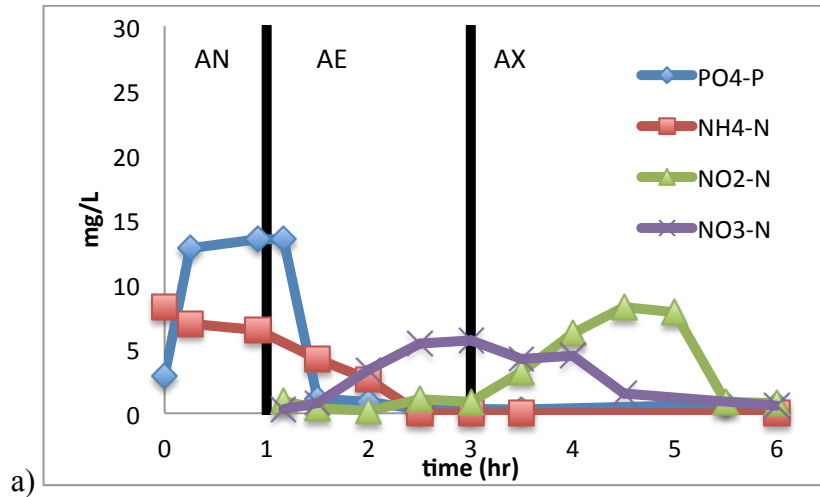


Figure 19: BIOPHO-PX 3 on a) 2/16/15, b) 3/7/15 and c) 3/16/15, and d) Average BIOPHO-PX 3 Phosphorous and Nitrogen across the cycle n=3

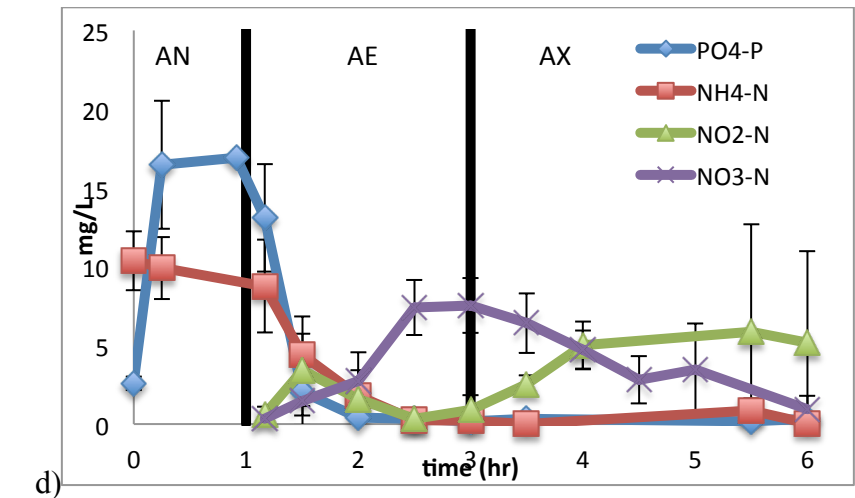
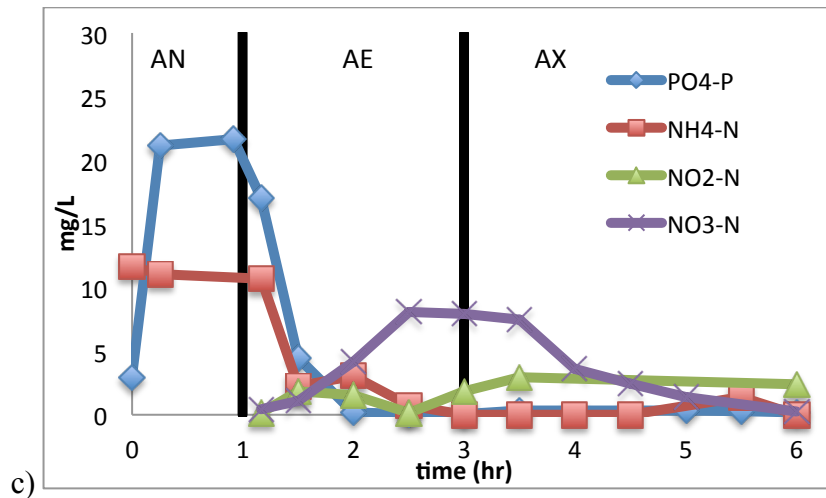
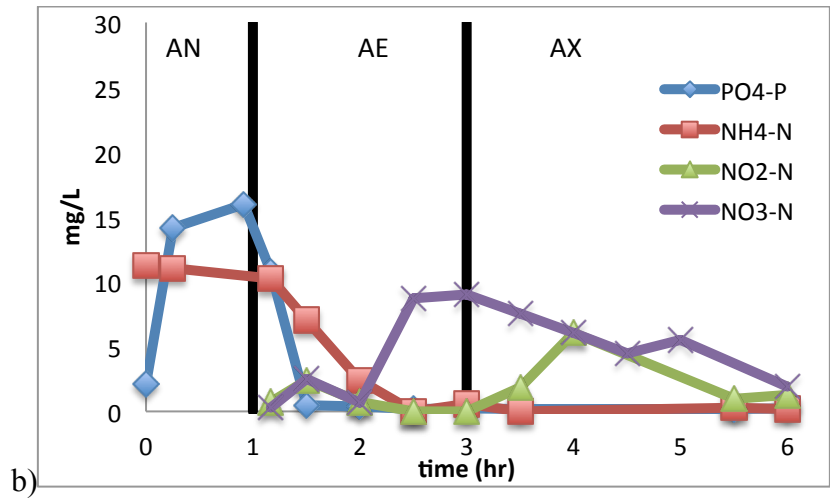
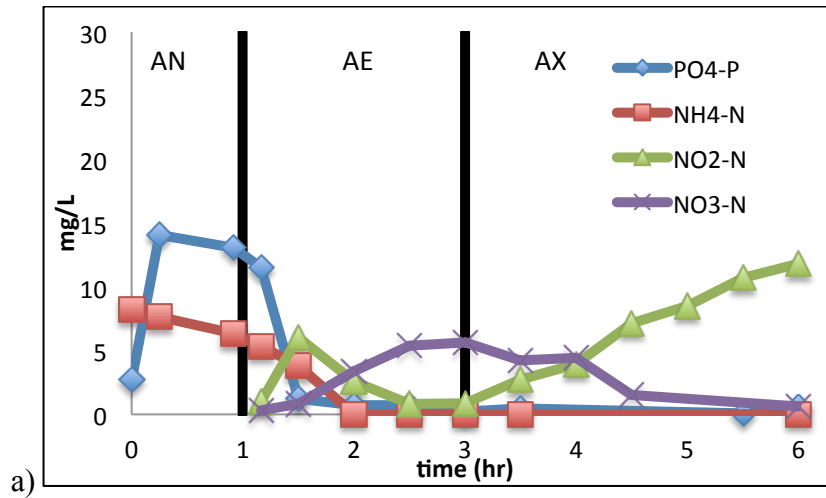


Figure 20 a-d: BIOPHO-PX 4 on 2/16/15, 3/7/15 and 3/16/15, and Average BIOPHO-PX 4 Phosphorous and Nitrogen across the cycle n=3

Table 13: Percent Removal for BIOPHO-PX Reactors at 20-day SRT

<b>n=3</b>	<b>Total P Removal (%)</b>	<b>Total N Removal (%)</b>	<b>NO<sub>2</sub>-N Accum. (end AE) (%)</b>
BIOPHO-PX 1	96.1 ± 1.8	16.0 ± 8.9	64.0 ± 18.6
BIOPHO-PX 2	97.0 ± 0.4	81.9 ± 10.5	40.4 ± 37.0
BIOPHO-PX 3	96.9 ± 1.7	79.3 ± 20.5	10.9 ± 10.0
BIOPHO-PX 4	97.8 ± 1.8	49.1 ± 42.7	10.7 ± 9.7

Table 14: qPCR data for BIOPHO-PX 1 through 4 at 20 day SRT

<b>n=2</b>	<b>% PAOs</b>	<b>%GAO</b>	<b>% AOBs</b>	<b>% NOBs</b>	<b>NOB/AOB</b>
BIOPHO-PX 1	74.1 ± 12.2	1.6 ± 0.82	0.3 ± 0.4	37.3 ± 15.5	124
BIOPHO-PX 2	54.7 ± 51.4	2.6 ± 0.6	0.7 ± 0.9	28.3 ± 10.9	40.4
BIOPHO-PX 3	12.1 ± 8.1	5.0 ± 1.7	0.6 ± 0.7	16.2 ± 1.8	27
BIOPHO-PX 4	17.4 ± 6.4	4.7 ± 2.7	0.4 ± 0.6	18.4 ± 15.2	46

### 5.2.2 Phosphorous Removal for Reactors at 20-day SRT

Similar to the BIOPHO-PX reactors operating at a 10-day SRT, all 4 BIOPHO-PX reactors were able to achieve phosphorus removal. Figure 17 through Figure 20 show an anaerobic P release followed by total P removal in the aerobic environment; these results are consistent with previous BIOPHO-PX investigations (Winkler, Coats and Brinkman 2011, Coats, Mockos and Loge 2011). BIOPHO-PX 1 and 2 show P removal is complete after the first 0.5-hr of the aerobic environment, which is consistent with the complete usage of PHA in the system shown in Figure 21 and previous BIOPHO-PX research (Winkler, Coats and Brinkman 2011). BIOPHO-PX 3 and 4 show P removal is complete after the first 1-hr of the aerobic environment. BIOPHO-PX 1 and 2 have significantly higher PAO populations than BIOPHO-PX 3 and 4 (Table 14), which may be why BIOPHO-PX 1 and 2 can remove

phosphorous more quickly from the bulk solution. PHA was complete used in the first 30 minutes of the aerobic zone (Figure 22) this means that the PAOs must then use their glycogen stores to remove the remaining  $\text{PO}_4\text{-P}$  and therefore will have less carbon stores for nitrogen removal in the anoxic zone (Tsuneda, et al. 2006).

The amount of PAOs in the respective systems ranged from 12.1% to 74.1% (Table 14). As observed in the bioreactors operating at a 10-day SRT, the MLSS being enriched with a minimum of PAOs is sufficient to achieve good biological P removal (Li, Zhang and Sun 2014, Kuba, et al. 1994). As would be expected with an increase in SRT, the relative amount of PAOs in the system is much higher in the 20-day SRT reactor. The GAO percentage of the system remains small but has also a slight increase in the 20-day SRT reactors; this suggests that the extended SRT has selected for PAO growth without a significant increase in GAO growth, allowing for continued low P effluent.

As stated above, the P/C ratio is the measurement of phosphorous released in the anaerobic zone and the VFAs in the influent. This ratio is important for assessing whether or not the system has sufficient VFAs to remove the phosphorous. The P/C ratios were consistent with PAO-enriched cultures capable of performing EBPR, ranging from 0.17-0.5 (Winkler, Coats and Brinkman 2011, Oehman, Yuan, et al. 2005, Taya, et al. 2013, Carvalheira, et al. 2014, Liu, et al. 2013). Moreover, the P/C ratios increased from that observed at the 10-day SRT, which corresponded to lower effluent P values in the reactors.

**Table 15: Average MLSS concentrations for reactors with 20-day SRT n=3**

<b>Reactor</b>	<b>Average MLSS concentration (mg/L)</b>
BIOPHO-PX 1	2687 ± 379
BIOPHO-PX 2	3820 ± 245
BIOPHO-PX 3	4740 ± 492
BIOPHO-PX 4	3893 ± 273

Table 16: Influent VFA: and P ratios and Effluent P 20-day SRT

n=2,2,3,3	Influent VFA: Influent P (C mmol/Pmmol)	AN P release:VFA (P mmol/ C mmol)	Effluent P mg/L
BIOPHO-PX 1	20.6 ± 2.1	0.26 ± 0.08	0.6 ± 0.2
BIOPHO-PX 2	23.1 ± 5.2	0.26 ± 0.06	0.5 ± 0.2
BIOPHO-PX 3	24.2 ± 5.3	0.24 ± 0.05	0.5 ± 0.2
BIOPHO-PX 4	25.6 ± 4.6	0.25 ± 0.06	0.3 ± 0.2

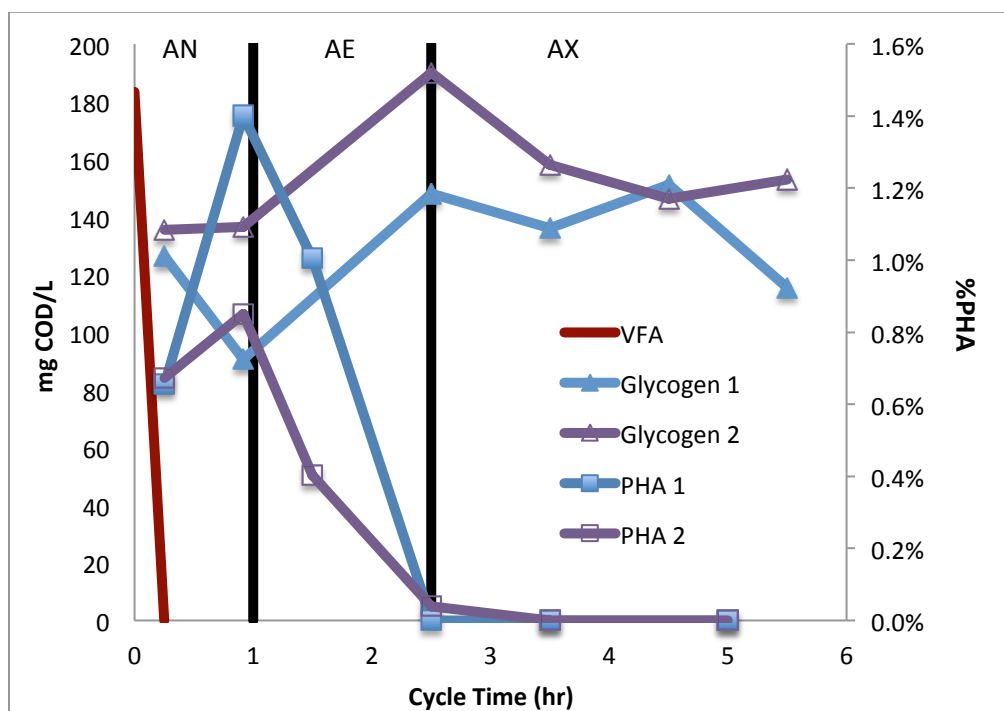


Figure 21: Carbon in BIOPHO-PX1 and 2

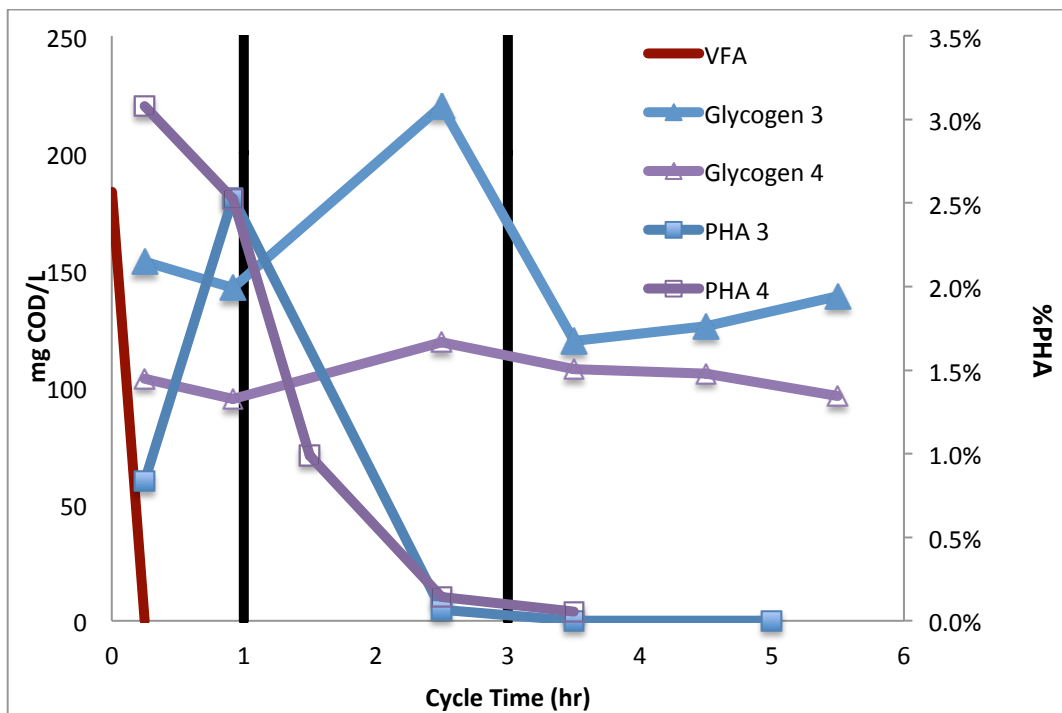


Figure 22: Carbon in BIOPHO-PX 3 and 4

### 5.2.3 DO Analysis for Reactors at 20-day SRT

The addition of second aquarium pump was made to the operational set-up to decrease the amount of time it took for the reactors to reach the residual DO concentration setpoint. As a consequence, this increase in the amount of air/oxygen applied to the system likely was the cause of enhanced nitrification, rather than nitrification, in the reactors.

DO curves versus time were recorded on each reactor most days of the operating cycles. Figure 23 shows a typical DO curves that were recorded for the 20-day SRT reactors. As shown and as expected, the lag time in achieving the target DO significantly decreased for all of the reactors (compared with the 10 day SRT operations; Figure 16), so that on average it was significantly less than 20 minutes. The average residual DO concentrations remained similar to those from the 10-day SRT reactors, i.e. the concentrations for BIOPHO-PX 1 and 3 are slightly higher than the setpoint while BIOPHO-PX 2 and 4 actual concentrations are

slightly lower than the setpoint. This consistency in the DO patterns shows the limitations of the DO control operations the current BIOPHO-PX system has and the DO concentrations it is capable of maintaining.

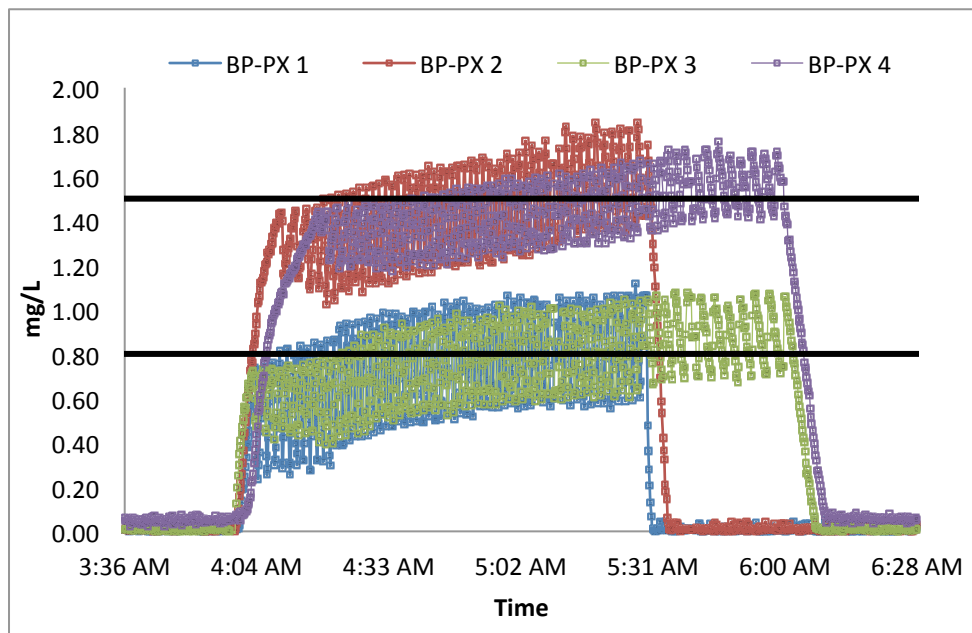


Figure 23: DO Profile across the aeration period for the BIOPHO-PX reactors 3/6/15

Table 17: Average Residual DO Concentrations and Time at Residual DO for BIOPHO-PX reactors at 20-day SRT

n=6	BIOPHO -PX 1	BIOPHO -PX 2	BIOPHO -PX 3	BIOPHO -PX 4
Avg. Residual DO (mg/L)	$0.74 \pm 0.01$	$1.43 \pm 0.03$	$0.77 \pm 0.02$	$1.46 \pm 0.03$
Time at Residual DO (min)	$85 \pm 4$	$76 \pm 13$	$111 \pm 9$	$99 \pm 8$

#### 5.2.4 20-day SRT Specific Rates

Table 18 shows the specific rates of phosphorus (P) release, phosphorus removal, ammonia oxidization and denitrification (SDNR) for the BIOPHO-PX reactors. As stated above, specific rates are calculated by normalizing the concentration of the species of interest

during a specific time interval by dividing by the MLSS concentration. BIOPHO-PX1 has the highest specific rates of P release and P uptake, this reactor also has the highest TP and therefore is the most efficient at P removal at its DO and aeration length settings. BIOHO-PX 2, 3, and 4 had comparable specific rates of P release and removal and performed as expected but not as well as BIOPHO-PX 1. BIOPHO-PX 2 has the largest TNR, which corresponds to the highest rate of ammonia oxidation and SDNR. This reactor is therefore most efficient at nitrogen removal. As with the 10-day SRT reactors, these SNDR values are highest than expected if the carbon used for denitrification was simply endogenous decay and also higher than previous SNDRs using this post-anoxic configuration, suggesting a larger carbon savings in the microorganisms (Metcalf and Eddy 2014, Winkler, Coats and Brinkman 2011).

**Table 18: 20-day SRT specific rates**

<b>n=1 or 3</b>	<b>P Release AN (mg P/ gVSS*hr)</b>	<b>P Removed AE (mg P/ gVSS*hr)</b>	<b>NH4 Oxidized (mg N/ g VSS *hr)</b>	<b>SDNR (mg NO<sub>x</sub>- N/gVSS*hr)</b>
BIOPHO-PX 1	5.38 ± 1.89	4.27 ± 1.27	0.72 ± 0.44	0.88 ± 0.94
BIOPHO-PX 2	3.92 ± 0.97	3.08 ± 0.73	1.73 ± 0.44	1.83 ± 0.64
BIOPHO-PX 3	2.81 ± 0.67	1.67 ± 0.38	0.89 ± 0.20	0.59 ± 0.44
BIOPHO-PX 4	3.67 ± 1.08	2.13 ± 0.60	1.13 ± 0.28	0.21 ± 0.87

### 5.2.5 Summary and Conclusions for Reactors at 20-day SRT

In summary, operating at a 20 day SRT the operational conditions for BIOPHO-PX 1 was not capable of achieving nitrogen removal and therefore is not candidate operational criteria for the BIOPHO-PX process. BIOPHO-PX 3 and 4 were over aerated so that

nitrification was fully achieved. These two reactors' operational criteria exceed the aeration needs for nitritation control. BIOPHO-PX 2 shows the most value for system optimization at the 20 day SRT.

## Chapter 6: Conclusions

### 6.1 Operational Recommendations

Considering the operational parameters applied and investigated in this study, there were two configurations that could be further optimized for the BOPPHO-PX process as related to achieving enhanced nitrification control: BIOPHO-PX 4 with a 10-day SRT and BIOPHO-PX 2 with a 20-day SRT. The MLSS enriched in these two reactors were able to completely oxidize the influent ammonia and performed EBPR, while sustaining some partial nitrification. These two reactors should be investigated further in order to optimize their performance so that nitrate formation does not occur and effluent phosphorus reaches 0.2mg/L or less.

Regarding BIOPHO-PX 4 with a 10-day SRT, this reactor can be optimized to perform nitrification by turning off the air when the residual DO has been reached, as this corresponds with onset of nitrate formation. The use of online  $\text{NO}_2$  and  $\text{NO}_3$  or  $\text{NO}_x$  sensors would be useful for nitrification control: air could be supplied until the  $\text{NO}_2$  sensor begins to detect a decrease in concentration and/or the  $\text{NO}_3$  or  $\text{NO}_x$  sensors begin to detect a larger increase than the  $\text{NO}_2$  sensor. EBPR for this reactor could be enhanced with an increase the P/C ratio by an increase of influent VFAs to the system.

Alternatively, BIOPHO-PX 2 with a 20-day SRT could also be optimized for nitrification by reducing the air supplied to the system to inhibit nitrification. This reduced air supply could then increase the lag time between nitrite and nitrate formation so that it more closely resembles BIOPHO-PX 4 with a 10-day SRT. If this lag is achieved, then the above mentioned monitoring scheme could be used to control for nitrification.

## **6.2 Energy Savings with Operational Recommendations**

As stated, one of the goals of the BIOPHO-PX research group is to reduce the energy demands and associated operational costs of a WRRF. A standard BNR plant (residual DO concentration typically set at a minimum of 2.0 mg/L, and upwards of 3.0 mg/L when nitrification is desired) requires an estimated 8.35 MW-hr per 10 million gallons of wastewater treated; aeration accounts for 5.46 MW-hr, or 65%, of the required energy (Coats, Watkins and Kranenburg 2011). If the operation scheme recommended herein is implemented at a full scale treatment plant, the residual DO would be reduced to 1.5 mg/L, which is a 25% decrease (minimum) in DO requirements. This would result in the aeration energy required per 10 million gallons to be reduced to 5.10 MW-hr and the total energy requirements to be decreased to 7.89 MW-hr. A standard WRRF would have an aerobic hydraulic retention time of 4 hrs. With either of these configurations recommended the aeration hydraulic retention time would be reduced to 2 hours; resulting in half of the aeration needed for the BIOPHO-PX process and the aeration energy demand being further reduced to 2.55 MW-hr, with the overall energy demand to 5.34 MW-hr. With the average cost of electric being 5.93 cents/kW-hr (Corporation 2015), there is a potential for an average annual savings of \$1,526,280 for the WRRF, compared to a typical BNR process.

## **6.3 Future Investigations**

The ultimate goal of the BIOPHO-PX process is to achieve complete nitritation, which would require either NOB washout or NOB inhibition. In this study, NOB washout as indicated by previous studies was not achieved in any reactor configuration. These previous studies that realized successful NOB washout (or near washout) had longer SRTs than applied herein, in the range of 30-68 days (Jubany, et al. 2009, Lemaire, Marcelino and Yuan

2008). With the current BIOPHO-PX setup, a longer SRT is not possible, as the reactor would overflow and/or be completely filled with biomass. If the reactors were scaled up, further SRT investigations would be possible which may achieve NOB washout.

Another possible investigation would be adjusting the residual DO concentration to achieve nitrification at a residual DO concentration lower than 0.8 mg/L, which would reduce the aeration costs to a WRRF even more than calculated in section 6.2. The reduced DO concentration has been shown to decrease the aeration costs in a WRRF. If it were possible to achieve nitrification at an even lower residual DO concentration, a WRRF could see even greater savings.

A final investigation of the BIOPHO-PX system would be the implementation of the system on a pilot scale model. The research group has a 3000 gallon (11356.2 L) scale model operating at the Moscow, ID WRRF that can be set up to model the BIOPHO-PX system as shown in Figure 4. This would allow for data collection on nitrification control in a continuous flow system, which is more common in municipal WRRFs.

## Works Cited

- Blackburne, Richard, Zhiguo Yuan, and Jurg Keller. "Partial nitrification to nitrite using low dissolved oxygen concentration as the main selection factor." *Biodegradation*, 2008: 303-312.
- Carvalho, Monica, Adrian Oehman, Gilda Carvalho, Mario Eusebio, and Maria A.M. Reis. "The impact of aeration on the competition between polyphosphate accumulating organisms and glycogen accumulating organisms." *Water Research*, 2014: 296-307.
- Clesceri, LS, AE Greenberg, and AD Eaton. *Standard Methods for Examination of Water and Wastewater*. 20. Washington D.C.: American Public Health Association, 1998.
- Coats, E.R., Z.T. Dobroth, and C.K. Brinkman. "EBPR using crude glycerol: Assessing process resiliency and exploring metabolic anomalies." *Water Environment Research*, 2013.
- Coats, Erik R., David L. Watkins, and Daniel Kranenburg. "A comparative Environment Life-Cycle Analysis for removing phosphorous from wastewater: biological versus physical/chemical." *Water Environment Research*, 2011.
- Coats, Erik., A. Mockos, and F.J. Loge. "Post-anoxic denitrification driven by PHA and glycogen within enhanced biological phosphorous removal." *Bioresource Technology*, 2011: 1019-1027.
- Corporation, Avista. *Servicing and Pricing Idaho Electric*. 2015.  
<https://www.avistautilities.com/services/energypricing/id/elect/Pages/default.aspx> (accessed April 23, 2015).
- Daigger, Glen T. "Oxygen and Carbon requirements for Biological Nitrogen Removal Processes Accomplishing Nitrification, Nitrification and Anamox." *Water Environment Research*, 2014: 204-209.
- Fang, Fang, Bing-Jie Ni, Xiao-Yan Li, Guo-Ping Sheng, and Han-Quing Yu. "Kinetic Analysis on the two-step process of AOB and NOB in aerobic nitrifying granules." *Applied Microbiology and Biotechnology*, 2009: 1159-1169.
- Fitzgerald, Colin M., Pamela Camejo, J. Zachary Oshlang, and Daniel R. Noguera. "Ammonia-oxidizing microbial communities in reactors with efficient nitrification at low-dissolved oxygen." *Water Research*, 2015: 38-51.
- Grady Jr, C.P. Leslie, Geln T. Daigger, Nancy G. Love, and Carlos D.M. Filipe Filipe. *Biological Wastewater Treatment*. Boca Raton: CRC Press, 2011.
- Guo, J., Y. Peng, S. Yang, Y. Zheng, H. Huang, and Z. Wang. "Long term effect of dissolved oxygen on partial nitrification performance and microbial community structure." *Bioresource Technology*, 2009: 2796-2802.

- Guo, X., J.H Kim, S.K. Behera, and H.S. Park. "Influence of dissolved oxygen concentration and aeration time on nitrite accumulation in partial nitrification process." *Environmental Science Technology*, 2008: 527-534.
- Huang, Zhongua, Philip B. Gedalanga, Pitiporn Asvapathanagual, and Betty H. Olsen. "Influence of physicochemical and operational parameters on Nitrobacter and Nitrospira communities in an aerobic activated sludge bioreactor." *Water Research*, 2010: 4351-4358.
- Im, Jiyoel, Jonyoung Jung, Hyokwan Bae, Daeik Kim, and Kyungik Gil. "Correlation between nitrite accumulation and the concentration of AOB in a nitrification reactor." *Environmental Earth Science*, 2014: 289-297.
- Jubany, Irene, Javier Lafuente, Juan A. Baeza, and Julian Carrera. "Total and stable washout of nitrite oxidizing bacteria from a nitrifying continuous activated sludge system using automatic control based on Oxygen Uptake Rate Measurements." *Water Research*, 2009: 2761-2772.
- Kapagiannidis, A.G., I. Zafiriadis, and A. Aivasidis. "Comparison between aerobic and anoxic metabolisms of denitrifying-EBPR sludge: effect of biomass poly-hydroxyalkanoates content." *Biotechnology*, 2013: 227-237.
- Katipoglu-Yazan, Tugce, Emine Ubay Cokgor, and Derin Orhan. "Modeling sequential ammonia oxidation kinetics in enriched nitrifying microbial culture." *Chemical Technology and Biotechnology*, 2015: 72-79.
- Kuba, T, A Wachtmeister, M.C.M von Loosdrecht, and J.J. Heijnen. "Effect of nitrate on phosphorous release in biological phosphorous removal systems ." *Water Science Technology*, 1994: 263-269.
- Lee, Hansaem, and Zuwhansludges Yun. "Comparison of biochemical characteristics between PAOs and DPAOs." *Journal of Environmental Sciences*, 2014: 1340-1347.
- Lemaire, Romain, Marcos Marcelino, and Zhiguo Yuan. "Achieving the Nitrite Pathway Using Aeration Phase Length Control and Step-feed in an SBR Removing Nutrients from Abattoir Wastewater." *Biotechnology and Bioengineering* 100, no. 6 (2008): 1228-1236.
- Li, Huosheng, Shaoqi Zhou, Guotao Huang, and Bin Xu. "Achieving stable partial nitrification using endpoint pH control in an SBR treating landfill leachate." *Process Safety and Environmental Protection*, no. 92 (2014): 199-205.
- Li, Yongmei, Zou, Jinte, Lili Zhang, and Jing Sun. "Aerobic granular sludge for simultaneous accumulation of mineral phosphorous and removal of nitrogen via nitrite in wastewater." *Bioresource Technology*, 2014: 178-184.

- Liu, Gang, Xiangyang Xu, Laing Zhu, Shuo Xing, and Jianyu Chen. "Biological nutrient removal in a continuous anaerobic-aerobic-anoxic process treating synthetic domestic wastewater." *Chemical Engineering*, 2013: 223-229.
- Lopez-Vazquez, Carlos M., et al. "Modeling the PAO-GAO competition: Effects of carbon source, pH and temperature." *Water Research*, 2009: 450-462.
- Madigan, Michael T., and John M. Martinko. *Brock Biology of Microorganisms*. Upper Saddle River: Pearson Prentice Hall, 2006.
- Metcalf, and Eddy. *Wastewater Engineering*. New York, New York: McGraw-Hill Education, 2014.
- Oehman, Adrian, Raymond J. Zeng, Zhiguo Yuan, and Jurg Keller. "Anaerobic Metabolism of Propionate by Polyphosphate-Accumulating in Enhanced Biological Phosphorous Removal Systems.Orgnaisms ." *Wiley Periodicals, Inc*, January 2005.
- Oehman, Adrian, Zhiguo Yuan, Linda L. Blackall, and Keller Jurg. "Comparison of Acetate and Propionate Uptake by Polyphosphate accumulating organisms and Glycogen Accumulating Organisms." *Wiley Periodicals, Inc*, May 12, 2005.
- Regmi, Pusker, et al. "Control of aeration, aerobic SRT and COD input for mainstream nitrification/denitrification." *Water Research*, 2014: 162-171.
- Smulders, G.J.F., J. van der Meij, M.M.C. van Loosdrecht, and J.J. Heijnen. "Model of the anaerobic metabolism of the biological phosphorous removal process:stoichiometry and pH influence ." *Biotechnology and Bioengineering*, 2004: 461-470.
- Soejima, Koichi, Kazuma Oki, and Akihiko Terada. "Effects of acetate and nitrite addition on fraction of denitrifying phosphate-accumulating organisms and nutrient removal efficiency in anaerobic/aerobic/anoxic process." *Biosystems Engineering*, 2006: 305-313.
- Taher, Edris, and Kartik Chandran. "High-Rate, High-Yield Production of Methanol by Ammonia-Oxidizing Bacteria." *Environmental Science and Technology*, 2013: 3167-3173.
- Taya, Carlota, Vijay Kumar Garlapati, Albert Guisosola, and Juan A. Baeza. "The selective role of nitrite in the PAO/GAO competition." *Chemosphere*, 2013: 612-618.
- Tian, Wen-De, Wei-Guang Li, Hui Zhang, Xlao-Rong Kang, and Mark C.M. van Loosdrecht. "Limited filamentous bulking in order to enhance integrated nutrient removal and effluent quality." *Water Research*, no. 45 (2011): 4877-4884.
- Tsuneda, Satoshi, Takahi Ohno, Koichi Soejima, and Akira Hirata. "Simultaneous nitrogen and phosphorous removal using denitrifying phosphate-accumulating organisms in a sequencing batch reactor." *Biochemical Engineering Journal*, 2006: 191-196.

Winkler, Matt, Erik Coats, and Cynthia Brinkman. "Advancing post-anoxic denitrification for biological nutrient removal." *Water Research*, 2011: 6619-6230.

Zeng, W., Y. Zhang, L. Peng, Y. Li, and S Wang. "Control and optimization of nitrifying communities for nitritation from domestic wastewater at room temperatures." *Enzyme and Microbial Technology*, 2009: 226-232.

Zeng, Wei, Yingying Yang, Lei Li, Xiangdong Wang, and Yongzhen Peng. "Effect of nitrite from nitritation on biological phosphorous removal in a sequencing batch reactor treating domestic wastewater." *Bioresource Technology*, 2011: 6657-6664.

Zeng, Wei, Yue Zhang, Lei Li, Yongzhen Peng, and Shuying Wang. "Simultaneous nitritation and denitriation of domestic wastewater without addition of external carbon sources at limited aeration and normal temperatures." *Desalination and Water Treatment*, September 2010: 210-219.

Zielinksa, Magdalena, Kattarzyna Bernat, Agnieszka Cydzik-Kwiatkowska, Joanna Sobolewska, and Irena Wojnowska-Baryla. "Nitrogen removal from wastewater and bacterial diversity in activated sludge at different COD/N ratios and dissolved oxygen concentrations." *Journal of Environmental Sciences*, 2012: 990-998.